AD E301 262

AD A135 737

DNA 6187F

HIGH-EXPLOSIVE FIELD TESTS

Explosion Phenomena and Environmental Impacts

Kenneth E. Gould
Kaman Tempo
816 State Street (P.O. Drawer QQ)
Santa Barbara, California 93102

1 October 1981

Final Report for Period 1 October 1980—1 October 1981

CONTRACT No. DNA 001-79-C-0053

APPROVED FOR PUBLIC RELEASE;
DISTRIBUTION UNLIMITED.

THIS WORK WAS SPONSORED BY THE DEFENSE NUCLEAR AGENCY UNDER RDT&E RMSS CODE B344079464 Y99QAXSX36705 H2590D.

Prepared for

UNCLASSIFIED

SECURITY CLASSIFICATION OF THIS PAGE (When Data Entered)

REPORT DOCUMENTATION PAGE		READ INSTRUCTIONS BEFORE COMPLETING FORM
1. REPORT NUMBER DNA 6187F	2. GOVT ACCESSION NO. AD-A135737	3. RECIPIENT'S CATALOG NUMBER
4. TITLE (and Subtitle) HIGH-EXPLOSIVE FIELD TESTS Explosion Phenomena and Environmental Impacts		5. TYPE OF REPORT & PERIOD COVERED Final Report for Period 1 October 1980 — 1 October 1981
		6. PERFORMING ORG. REPORT NUMBER KT-81-004(R)
7. AUTHOR(s) Kenneth E. Gould		8. CONTRACT OR GRANT NUMBER(s) DNA 001-79-C-0053
9. PERFORMING ORGANIZATION NAME AND ADDRESS Kaman Tempo 816 State Street (P.O. Drawer QQ) Santa Barbara, California 93102		10. PROGRAM ELEMENT, PROJECT, TASK AREA & WORK UNIT NUMBERS Subtask Y99QAXSX367-05
11. CONTROLLING OFFICE NAME AND ADDRESS Director Defense Nuclear Agency Washington, D.C. 20305		12. REPORT DATE 1 October 1981
		13. NUMBER OF PAGES 90
14. MONITORING AGENCY NAME & ADDRESS(if different from Controlling Office)		15. SECURITY CLASS. (of this report) UNCLASSIFIED
		15a. DECLASSIFICATION/DOWNGRADING SCHEDULE NA since UNCLASSIFIED

16. DISTRIBUTION STATEMENT (of this Report)

Approved for public release; distribution unlimited.

17. DISTRIBUTION STATEMENT (of the abstract entered in Block 20, if different from Report)

18. SUPPLEMENTARY NOTES

This work was sponsored by the Defense Nuclear Agency under RDT&E RMSS Code B344079464 Y99QAXSX36705 H2590D.

19. KEY WORDS (Continue on reverse side if necessary and identify by block number)

High Explosives
Explosions
Airblast
Ground Shock
Environmental Impact

20. ABSTRACT (Continue on reverse side if necessary and identify by block number)

Methodologies are formulated to predict the magnitudes of high-explosive explosions phenomena for various high-explosive charge sizes and configurations and to relate these magnitudes to impacts on the natural physical and biological environment and on humans and the socioeconomic environment. The methodologies apply for the explosives normally used in land-based military high-explosive field tests, i.e., 0.5 to 500 tons of TNT-equivalent weight. The phenomena addressed include airblast and noise; craters and ejecta and missiles; ground shock; and explosion clouds of chemical products and dust.

DD FORM 1 JAN 73 1473 EDITION OF 1 NOV 65 IS OBSOLETE

UNCLASSIFIED

SECURITY CLASSIFICATION OF THIS PAGE (When Data Entered)

TABLE OF CONTENTS

LIST OF ILLUSTRATIONS

Figure		Page
2-1	Peak airblast overpressure measurements from large TNT explosions.	9
2-2	Airblast peak overpressures versus ground distance for charges exploded on or near the ground surface.	10
2-3	Long-distance airblast and noise.	11
2-4	Height-of-burst multiplying factor.	15
2-5	Crater volumes from 256-pound spheres of TNT in dry alluvium.	16
2-6	Near-surface HE cratering efficiencies.	19
2-7	Normalized cratering efficiency for various geologies.	20
2-8	Near-surface HE cratering efficiency in wet geologies.	22
2-9	Near-surface HE cratering efficiency in dry soil.	23
2-10	Near-surface HE cratering efficiency in dry soft rock.	24
2-11	Near-surface HE cratering efficiency in dry hard rock.	25
2-12	Crater radii and depths as functions of crater volume.	26
2-13	Dimensionless plot of ejecta mass density as a function of range.	28
2-14	Ground motions from previous large HE field tests.	29
2-15	Maximum expected ground motions from near-surface explosions.	31
2-16	Height aboveground of large-explosion clouds.	34
2-17	Diameters of large-explosion clouds.	36
2-18	Top of MISERS BLUFF clouds.	37
2-19	Diameter of MISERS BLUFF clouds.	37

LIST OF TABLES

Table		Page
1-1	Unit conversion factors.	6
2-1	TNT-equivalent weights of explosives for airblast peak overpressure.	8
2-2	TNT-equivalent weights of explosives for ground cratering.	17
2-3	HE cratering efficiency for generic geologic materials.	26
2-4	Ideal explosion products, given in percent by weight.	32
3-1	Summary of estimates of lethality due to translation by airblast and impact against a hard surface.	48
3-2	Summary of airblast damage threshold levels.	57
3-3	Modified Mercalli Intensity Scale of 1931.	61
3-4	Soviet Union explosion-induced ground motion criteria.	64
3-5	Ground motion measurements near RULISON nuclear underground test.	66
3-6	Building count and damage data from RULISON ground motions.	66
3-7	Human response to ground motions.	70

SECTION 1

INTRODUCTION

Section 3 describes the magnitudes of explosion phenomena that may have significant effects on the environment and combines these damage criteria with the explosion phenomena in Section 2 to obtain damage distances or conditions, i.e., distances within, or other conditions for, which the effects of explosion phenomena can be significant.

A variety of units of measurement is used in this report, depending on how particular types of data are customarily given. In general, however, information in output form for users of this manual is presented in metric units, except HE charge sizes are given in TNT-equivalent tons. Table 1-1 shows the factors to convert to other measurement systems.

Table 1-1. Unit conversion factors.

To Convert	Into	Multiply By
[illegible]	[illegible]	[illegible]

SECTION 2

EXPLOSION PHENOMENA

The detonation of a charge of high explosive (HE) near the earth's surface produces airblast and noise, a crater, ejecta and missiles, ground shock, explosive products, and a buoyant cloud that will carry dust and explosive products downwind. In this section, the magnitudes of each of these phenomena are estimated for explosive charge weights ranging from 1,000 pounds to 500 tons (typical for field tests) exploded on or near the ground surface. The variation of magnitude of phenomena for special situations (e.g., multiple charges and elevated or buried charges) is also discussed.

In this report, all weights of explosives are given in terms of their TNT-equivalent weight, i.e., the weight of TNT (with explosive energy of 10^9 calories/ton) that would produce approximately the same magnitude of a particular phenomenon as the specific explosive charge in question.

AIRBLAST AND NOISE

Airblast (the explosion shock wave in air) is usually of greatest concern in HE field tests because damage can occur at relatively long distances from the explosion. Damage can be caused by various airblast mechanisms but is usually related to the peak overpressure of the airblast wave. Table 2-1 shows TNT-equivalent weight factors for some explosives. The airblast phenomena discussed in this section include close-in airblast, long-distance airblast and noise, and refracted atmospheric propagation.

Close-In Airblast

Figure 2-1 shows measured values of airblast peak overpressure as functions of distance for four field tests in which large, spherical charges of TNT were detonated on the ground surface. The measurements have been adjusted to convert all results to 1 pound of TNT at sea level and standard atmospheric conditions. It can be seen that these results agree very well and were predictable.

Airblast measurements from a number of charges of various shapes (sphere, hemisphere, and capped cylinder), varying in TNT-equivalent weight from a few hundred pounds to 500 tons and employing different types of explosives, show results consistent with Figure 2-1 in the region of environmental interest, below 10 to 20 psi (References 3, 4, 5, and 6). Also, except for charges elevated significantly above the earth's surface (at least tens to hundreds of feet for charge sizes of interest), Figure 2-1 is a slightly conservative estimate of airblast overpressure. Field tests

Table 2-1. TNT-equivalent weights of explosives for airblast peak overpressure. (Source: Reference 1)

Explosive Type	TNT-Equivalent Weight Factor[a]	Explosive Type	TNT-Equivalent Weight Factor[a]
TNT	1.00	Pentolite	1.42
Tritonal	1.07	PETN	1.27
Composition B	1.11	Nitroglycerine	1.23
HBX-1	1.17	RDX-Cyclonite	1.17
HBX-3	1.14	Nitromethane	1.00
TNETB	1.36	Ammonium Nitrate	0.84
Composition C-4	1.37	Black Powder	0.46
H-6	1.38		

[a]To determine the TNT-equivalent weight of an explosive, multiply the weight of the explosive by the equivalent weight factor, e.g., at a given distance, 1 ton of ammonium nitrate is required to produce the peak overpressure equivalent to that from 0.84 ton of TNT.

conducted at higher altitudes result in peak overpressures somewhat less than those indicated in Figure 2-1. Burying a charge tends to also reduce the peak overpressures. Thus it can be assumed that except for significantly elevated charges (discussed later), the airblast overpressure will not be greater than indicated by Figure 2-1.

The distance at which any particular peak overpressure occurs varies proportional to the cube root of the charge weight, e.g., increasing a charge weight by a factor of 8 increases the ground distance for a given overpressure by a factor of $8^{1/3}$, i.e., 2. The curves shown in Figure 2-2 for typical weights of field test HE charges are obtained from Figure 2-1 by plotting overpressures of environmental concern (below 20 psi or 140 kPa) versus the product of ground distance and the cube root of the charge weight.

Long-Distance Airblast

As the peak overpressure decreases at increasing distances from the explosion, the airblast front slows down to a speed approaching the speed of sound. As the airblast approaches an acoustic wave, it is refracted by temperature and wind-speed gradients in the air. At distances where the airblast peak overpressure is less than approximately 2.5 kPa, meteorological conditions usually predominate to cause anomalous propagation; airblast

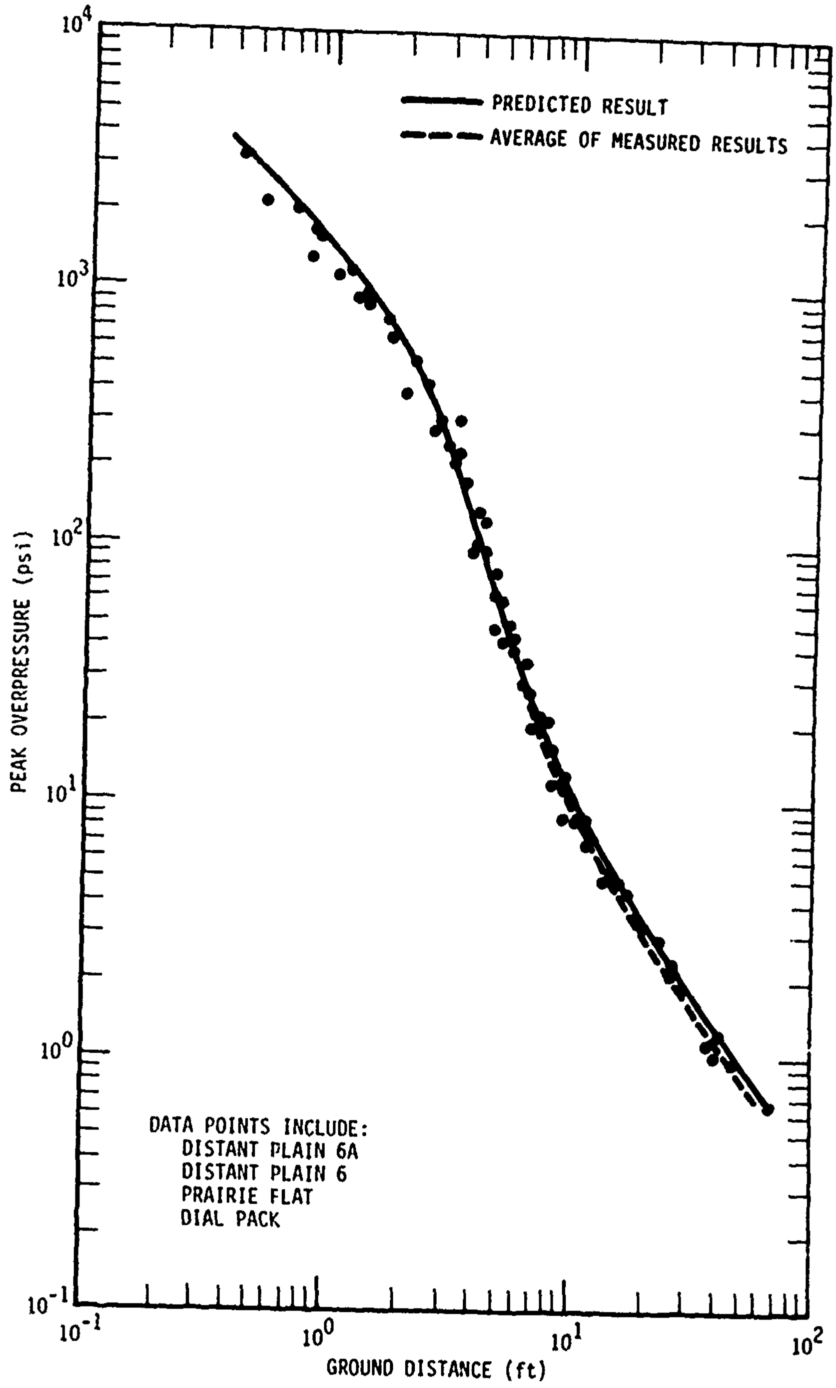

Figure 2-1. Peak airblast overpressure measurements from large TNT explosions (scaled to 1 pound of TNT at sea level and standard atmospheric conditions). (Source: Reference 2)

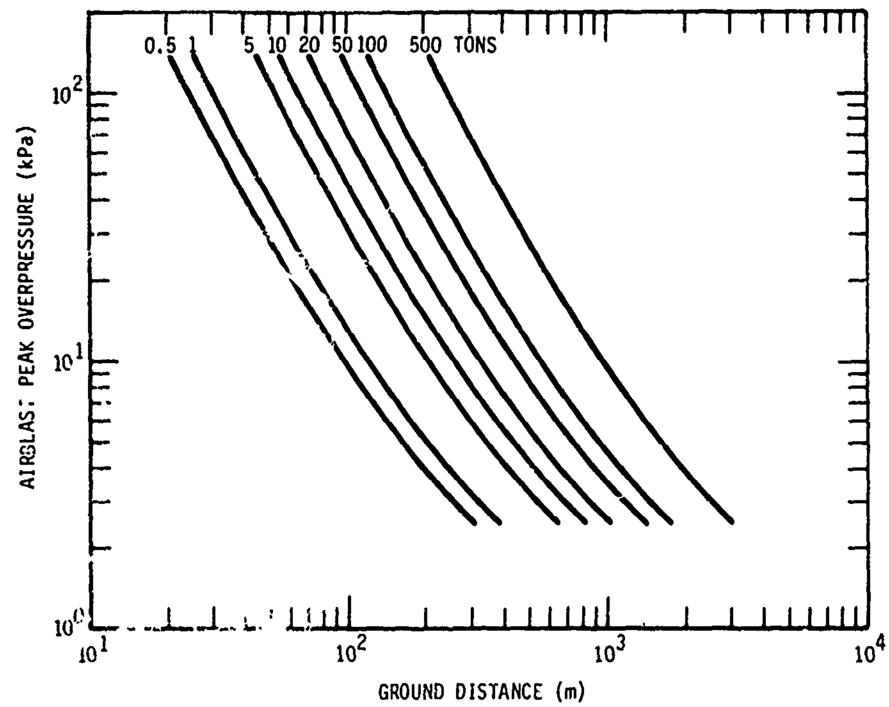

Figure 2-2. Airblast peak overpressures versus ground distance for charges exploded on or near the ground surface.

is refracted toward or away from the ground, resulting in peak overpressures either greater or less than would occur in a nonrefracting atmosphere. Peak overpressures at long distances may vary by an order of magnitude or more, depending upon whether the meteorological conditions are favorable or unfavorable. Long-distance airblast is of concern because very low peak overpressures can crack windows and cause excessive noise, as discussed in Section 3.

Based on a large amount of empirical data, Reed (Reference 1) has formulated relationships for estimating the overpressure at long distances from explosions. For a large chemical explosion on, or near, the ground surface with the airblast propagating through a homogeneous, nonrefracting atmosphere, the peak overpressure at long distances near the ground surface is approximately:

$$\Delta p = 668\ (2W)^{0.37}\ D^{-1.1}\ (P/P_0)^{0.63} \qquad (2\text{-}1)$$

where

Δp = incident peak overpressure (Pa)

W = TNT-equivalent weight of the explosive charge (tons) (the factor of 2 is to account for the fact that the ground surface produces distant blast pressures equivalent to those from a free-air burst about double in size)

D = distance from the explosion (km)

Noise

An explosion produces impulsive, predominantly low-frequency sound of sufficient intensity to be heard at long distances. The measure of sound intensity is the unweighted sound pressure level (SPL) expressed in decibels (dB), which are dimensionless units proportional to the square of the pressure ratio (relative to a reference pressure of 2×10^{-5} Pa). The equation is:

$$SPL(dB) = 20 \log (\Delta p/0.00002) = 20 \log (\Delta p) + 94 \qquad (2\text{-}2)$$

where Δp = peak pressure change in Pa. The sound pressure levels in decibels are shown on the right-hand scale of Figure 2-3.

Explosive charges produce a sound energy spectrum that is predominantly low frequency at distances of interest, approximately 10 hertz (Hz) or less for large charges. The energy concentration is displaced toward the low end as explosive yield increases. Also at greater distances, the spectrum is displaced toward lower frequencies as higher frequencies undergo greater

The meteorological conditions that lead to amplification of long-distance airblast and the relative location and magnitude of such amplification are summarized by Reed from a large amount of data (Reference 1). The three conditions of concern are boundary layer ducting, jet stream ducting and focusing, and downwind ozonosphere propagation.

In a temperature inversion, warm air overlies cooler air near the ground surface with the result that acoustic waves are trapped and ducted

Even a moderate amount of dirt cover will significantly reduce overpressure in the relatively high-overpressure region shown in Figure 2-2. However, there is little if any reduction in overpressures at long distances, shown in Figure 2-3, unless the depth-of-burst is relatively deep (Reference 7). In fact, exploding a charge at a shallow depth-of-burst may increase airblast magnitude at long distances because of more efficient conversion of explosive energy to shock energy when an explosion is confined (Reference 8). The assumption of no reduction in airblast or noise from burying a charge is usually warranted for environmental assessment. If this assumption indicates that significant environmental damage may occur from close-in airblast and if the depth-of-burst is deeper than about one charge radius, it may be desirable to have the airblast phenomena calculated by a specialist who can include depth-of-burst effects.

When a charge is exploded above the ground surface, shock waves reflected from the ground surface merge with the direct shock wave to enhance the magnitude of the peak overpressure at any given distance. As shown in Figure 2-4, the effect of elevating a charge is to make it appear that the charge is increased in weight. At the optimum height-of-burst for airblast enhancement, a charge appears to be increased in weight approximately 3.5 times so that the distance to a given overpressure (by cube root scaling) is about 1.5 times that from a charge of the same weight exploded on the ground surface.*

Figure 2-4 can be used to estimate the increase in airblast magnitude for an elevated charge. The product of the TNT-equivalent charge weight and the multiplying factor should be used in Figures 2-2 and 2-3 to estimate the airblast magnitude as a function of distance. Substantial elevation is required to significantly extend the distance of a given peak overpressure, e.g., a 1-ton charge would have to be elevated approximately 60 feet above ground level to extend a given overpressure 10 percent farther.

If more than one charge is exploded at nearly the same location and time so that the shock waves interact, the airblast environment is complex. Outside the array of charges and depending on the distance, as was shown with the MISERS BLUFF multicharge event, the airblast may appear as a series of explosions or as a single explosion of larger size than any of the individual explosions. The conservative assumption for distant blast is that the individual shocks will merge to produce a single shock equivalent to that from a single charge with a weight equal to the sum of the weights of the individual charges and located at the center of the array.

---

* Height-of-burst is measured from the center of gravity of the explosive charge to the ground surface. Therefore, zero height of burst means the charge is half buried in the ground.

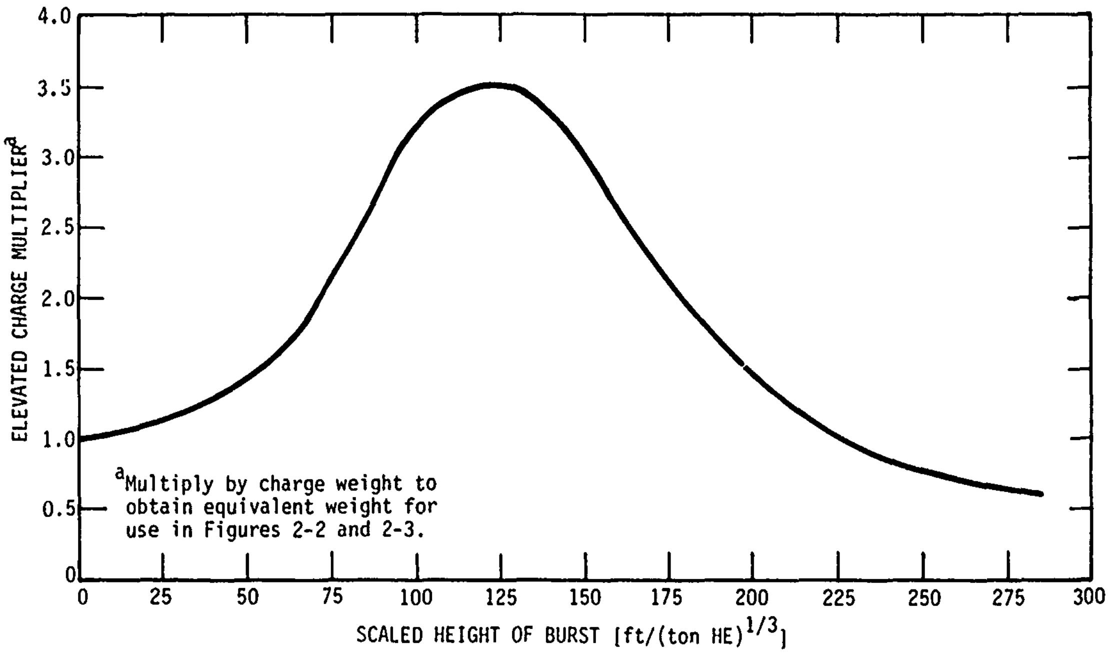

Figure 2-4. Height-of-burst multiplying factor. (Adapted from Reference 1)

CRATERS

The dimensions of an explosion-produced ground crater depend on a number of factors but are most strongly influenced by the TNT-equivalent weight of the charge, the placement of the charge relative to the ground surface, and the type of soil or rock and its water content. Crater dimensions are best predicted based on any previous explosions at the same test site, but even in this case crater dimensions can vary considerably under seemingly identical conditions. For example, PRE-DICE THROW I and II were both 100-ton TNT-equivalent HE charges at virtually the same location; yet, one crater was considerably shallower and wider than the other.

Figure 2-5 shows data for crater volumes from 256-pound spheres of TNT exploded on and below the ground surface in alluvium soils at two different sites.* As can be seen, crater volume increases with depth of charge burial to a maximum volume at the optimum depth for cratering, which is proportional to the charge weight and is about 10 feet for these 256-pound

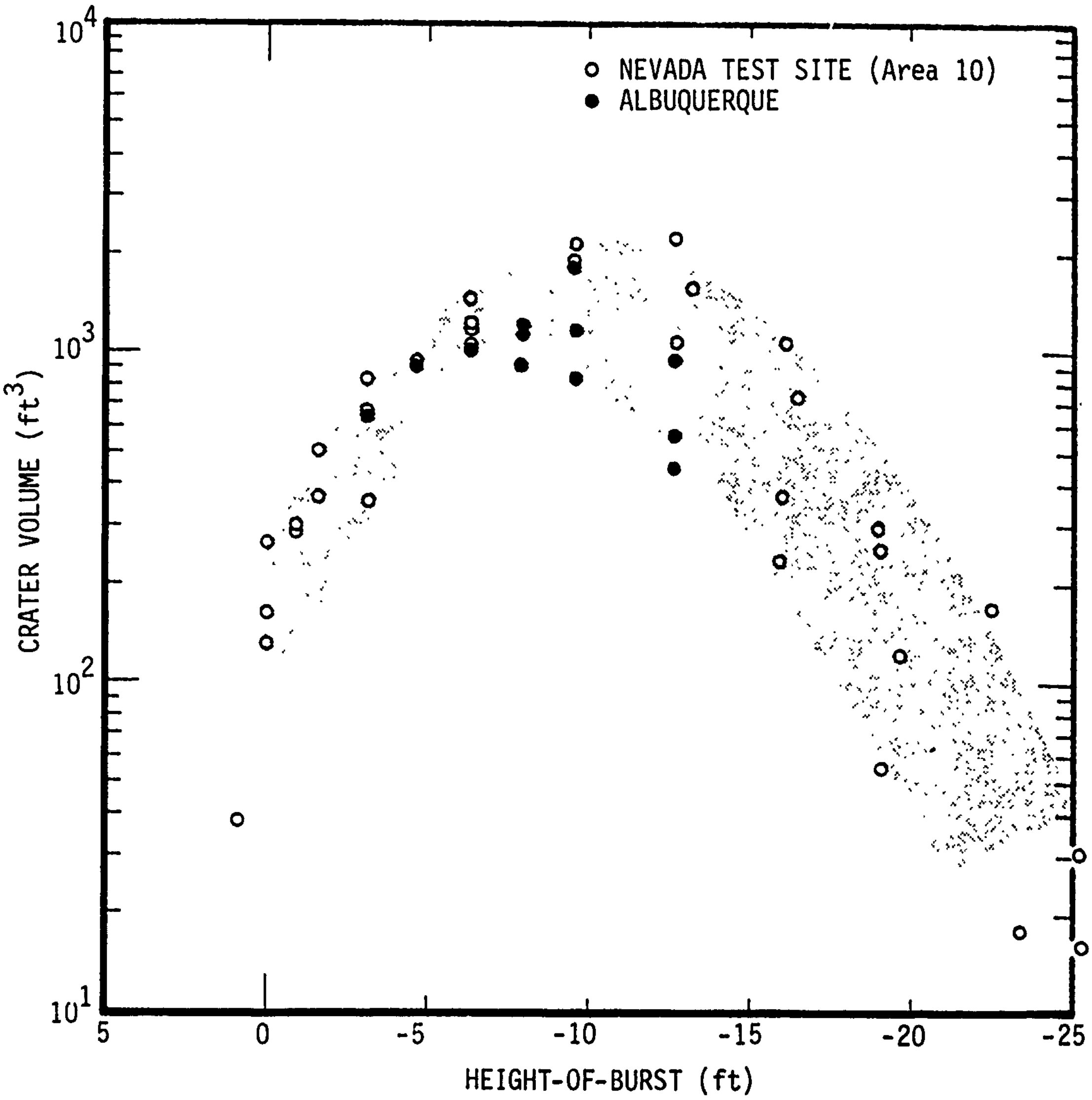

Figure 2-5. Crater volumes from 256-pound spheres of TNT in dry alluvium. (Source: Reference 9)

contained and crater volume decreases. If the charge is buried deep enough, it will be fully contained and no crater will be visible. Note that for relatively shallow-buried charges (those above the optimum cratering depth), the scatter of data indicates that crater volumes may differ by a factor of 2 or 3 for this specific situation, primarily from geological uncertainties. A different geological condition would result in a different set of data.

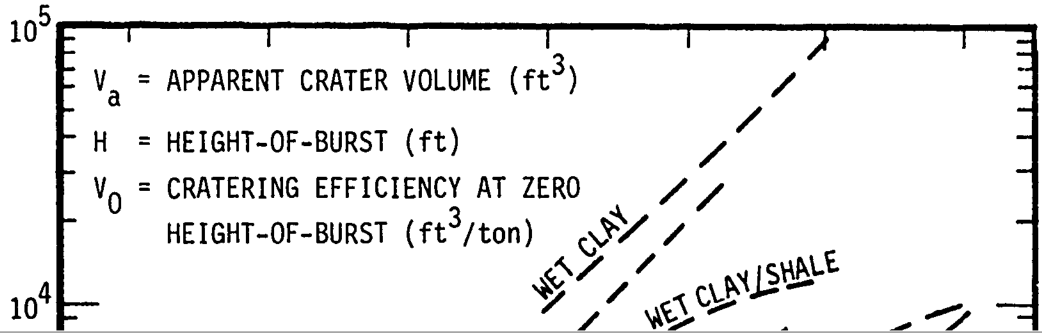

10^5
10^4
V_a = APPARENT CRATER VOLUME (ft^3)
H = HEIGHT-OF-BURST (ft)
V_0 = CRATERING EFFICIENCY AT ZERO HEIGHT-OF-BURST (ft^3/ton)
WET CLAY
WET CLAY/SHALE

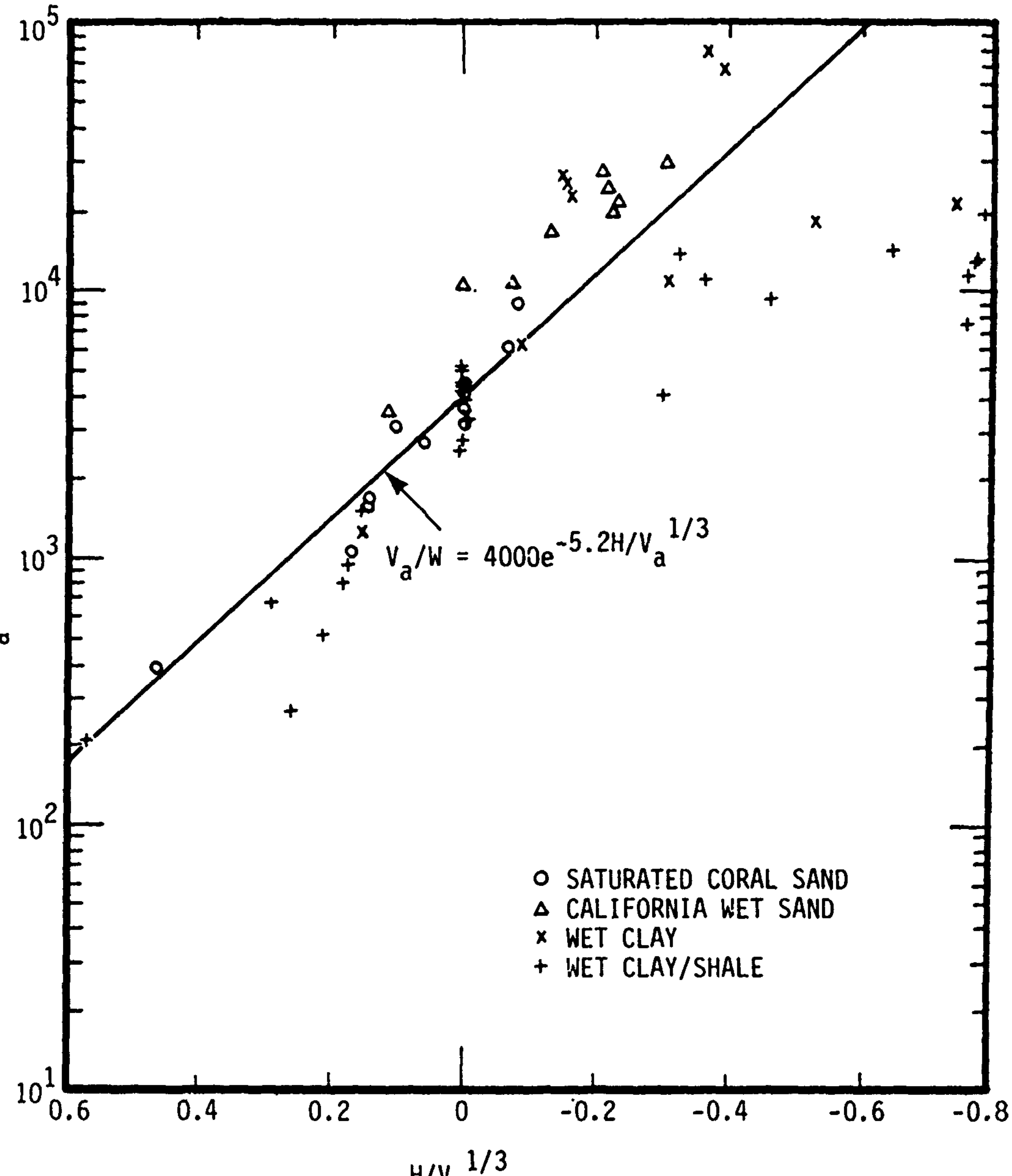

Figure 2-8. Near-surface HE cratering efficiency in wet geologies. (Adapted from Reference 9)

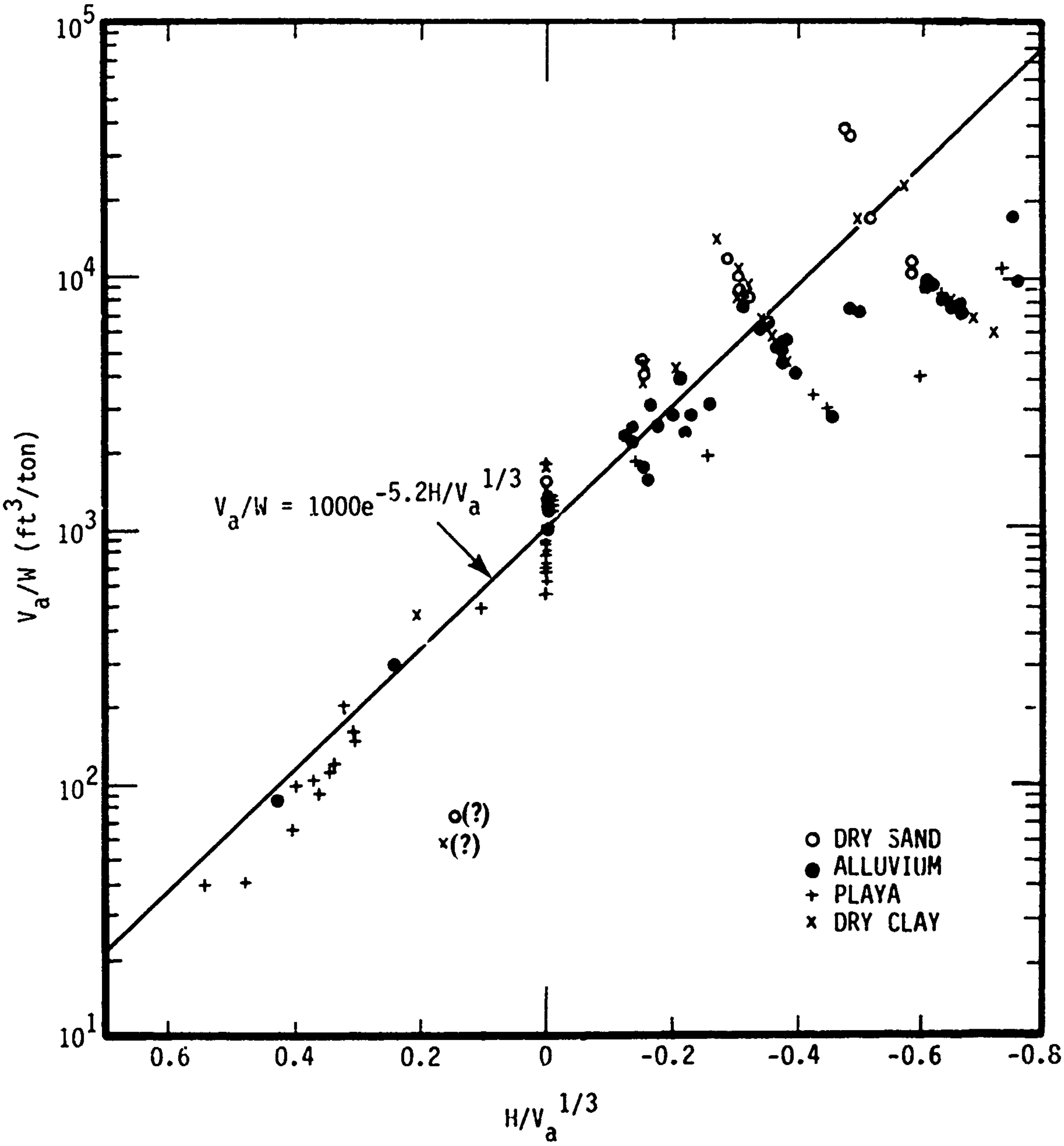

Figure 2-9. Near-surface HE cratering efficiency in dry soil. (Adapted from Reference 9)

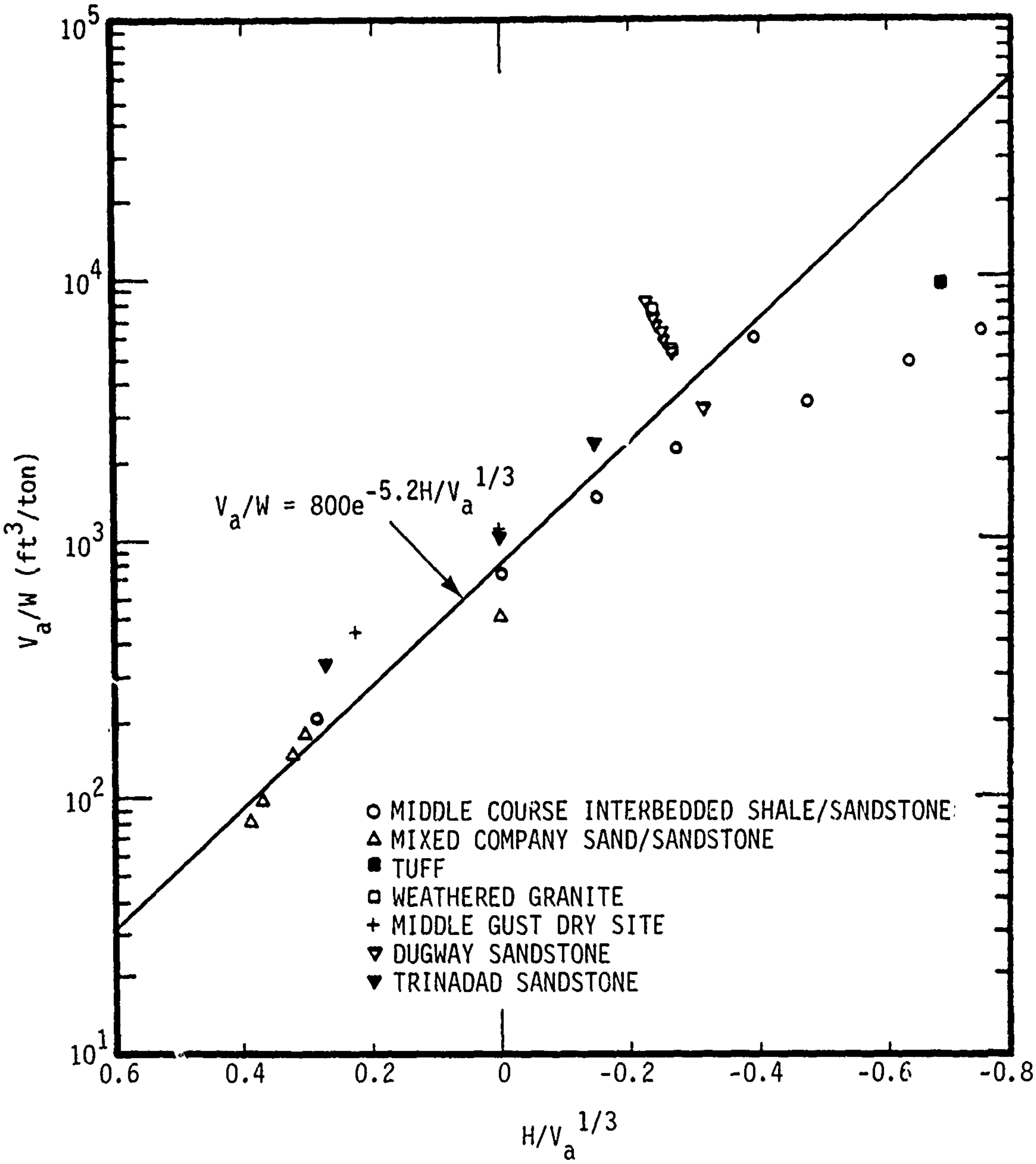

Figure 2-10. Near-surface HE cratering efficiency in dry soft rock. (Adapted from Reference 9)

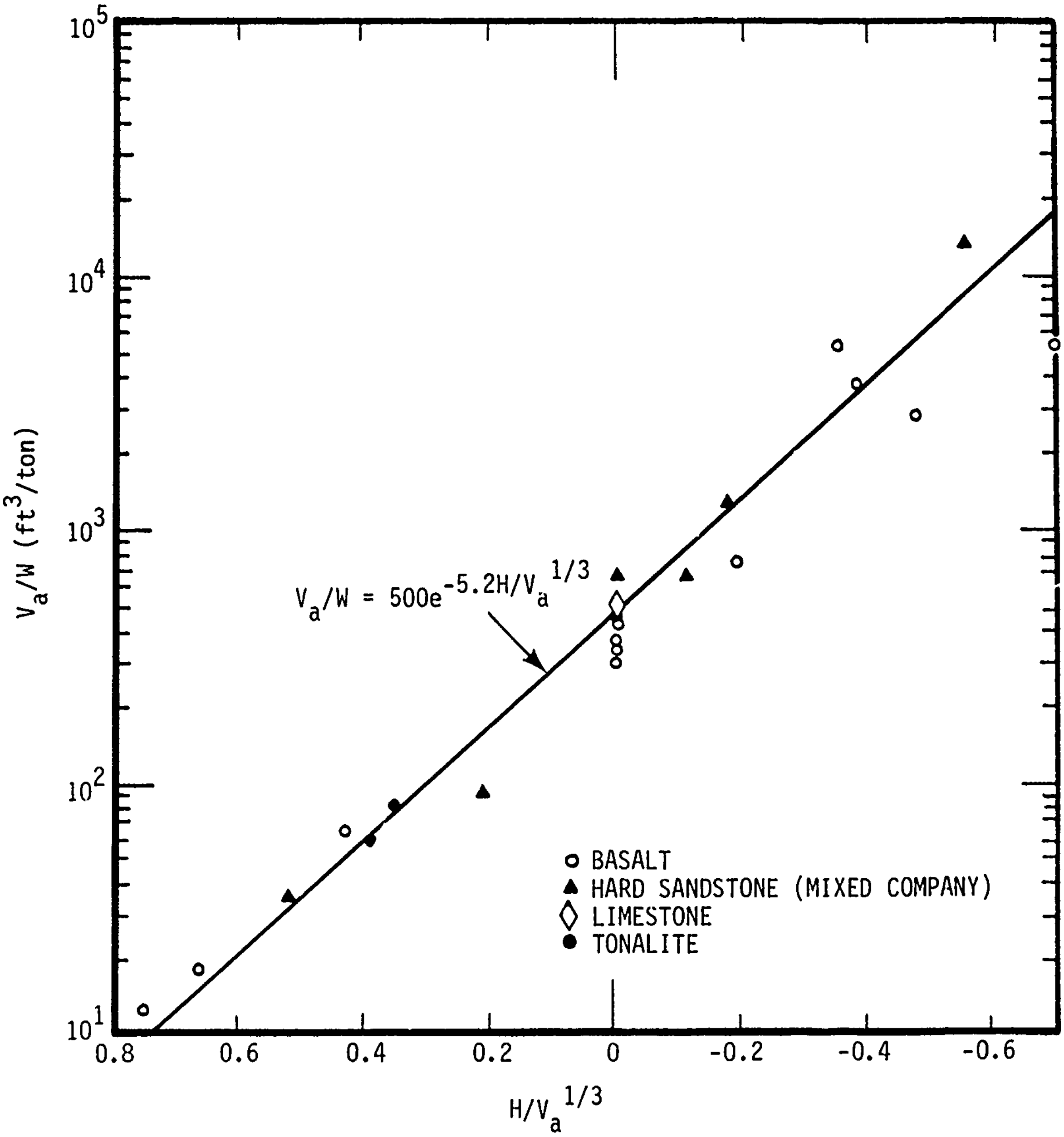

Figure 2-11. Near-surface HE cratering efficiency in dry hard rock. (Adapted from Reference 9)

Table 2-3. HE cratering efficiency for generic geologic materials. (Adapted from Reference 9)

Medium	V_0 (ft^3/ton) Range	Best Estimate
Wet Geology (including soils and clay shales)	2,000 to 8,000	4,000
Dry Soil	600 to 1,800	1,000
Dry Soft Rock	500 to 1,200	800
Dry Hard Rock	300 to 700	500

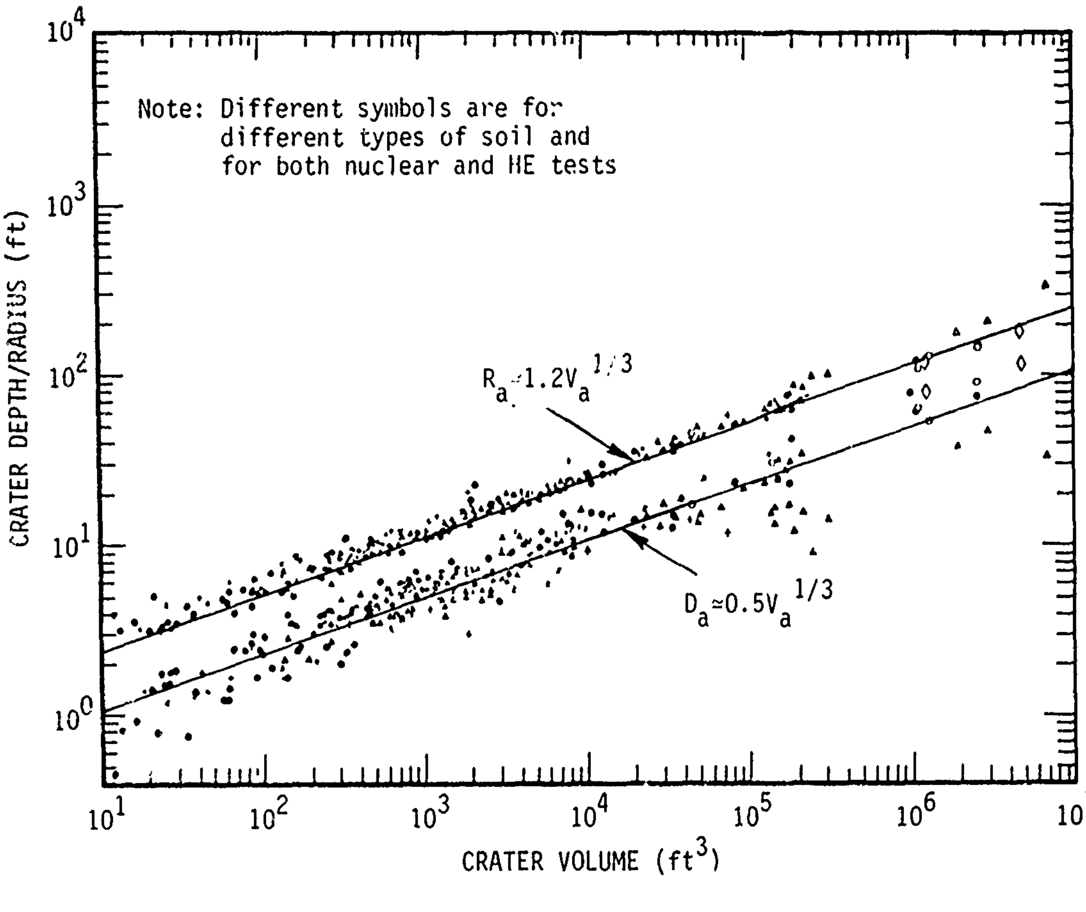

Figure 2-12. Crater radii and depths as functions of crater volume. (Adapted from Reference 9)

EJECTA AND MISSILES

Most of the ejecta, the earth materials from the apparent crater, from a large HE explosion are deposited within about 3 to 5 crater radii of ground zero (GZ), i.e., within a few hundred feet of a 500-ton charge. Beyond this distance, the ejecta do not completely cover the ground surface and the areal density decreases rapidly with increased distance from GZ.

The ground coverage of the ejecta can be estimated from Figure 2-13 as a function of crater dimensions and the density of earth materials. The unit weight of dry earth materials in-place varies, but reasonable values to use are 80 lb/ft^3 for porous earth, 90 lb/ft^3 for clay, 100 lb/ft^3 for sand, 120 lb/ft^3 for desert alluvium, 140 lb/ft^3 for soft rock, and 160 lb/ft^3 for hard rock.

Theoretically, some ejecta (missiles) can be propelled very long distances; in fact, however, very few missiles have been found beyond 3,000 feet from large HE explosions.

GROUND SHOCK

There are relatively few data on ground motion measurements from large HE field tests at distances of interest for environmental analysis, i.e., where the peak particle velocity is less than a few centimeters per second. Figure 2-14 shows the peak particle velocities from five HE field tests that had ground motion measurements at the magnitudes of interest. (All distances have been scaled to 1 ton of TNT by the cube root of the TNT-equivalent weight.) The three charges exploded either on the ground surface or, at most, just buried with the top of the charge flush with the ground surface (MIXED COMPANY III, JANGLE HE-2, AFWL 1-5) produced reasonably consistent ground motions, with the MIXED COMPANY III ground shock having the greatest magnitude. The more deeply buried charges in the ESSEX I--Phase 2 and PRE-GONDOLA--Shot B tests produced somewhat stronger ground shocks, as would be expected. In this study, the MIXED COMPANY III data will be assumed as the worst-case ground shock for near-surface explosions. Assuming that the maximum vertical, radial, and tangential peak particle velocities add vectorially,* the equation of the resultant peak ground motions can be expressed as follows:

$$V_{max} = 2,700\ (D/W^{1/3})^{-1.4} \qquad (2\text{-}6)$$

---

* The combined data are not given in the references, but adding the peak vectors results in the largest possible magnitudes of ground motion and therefore is a conservative assumption.

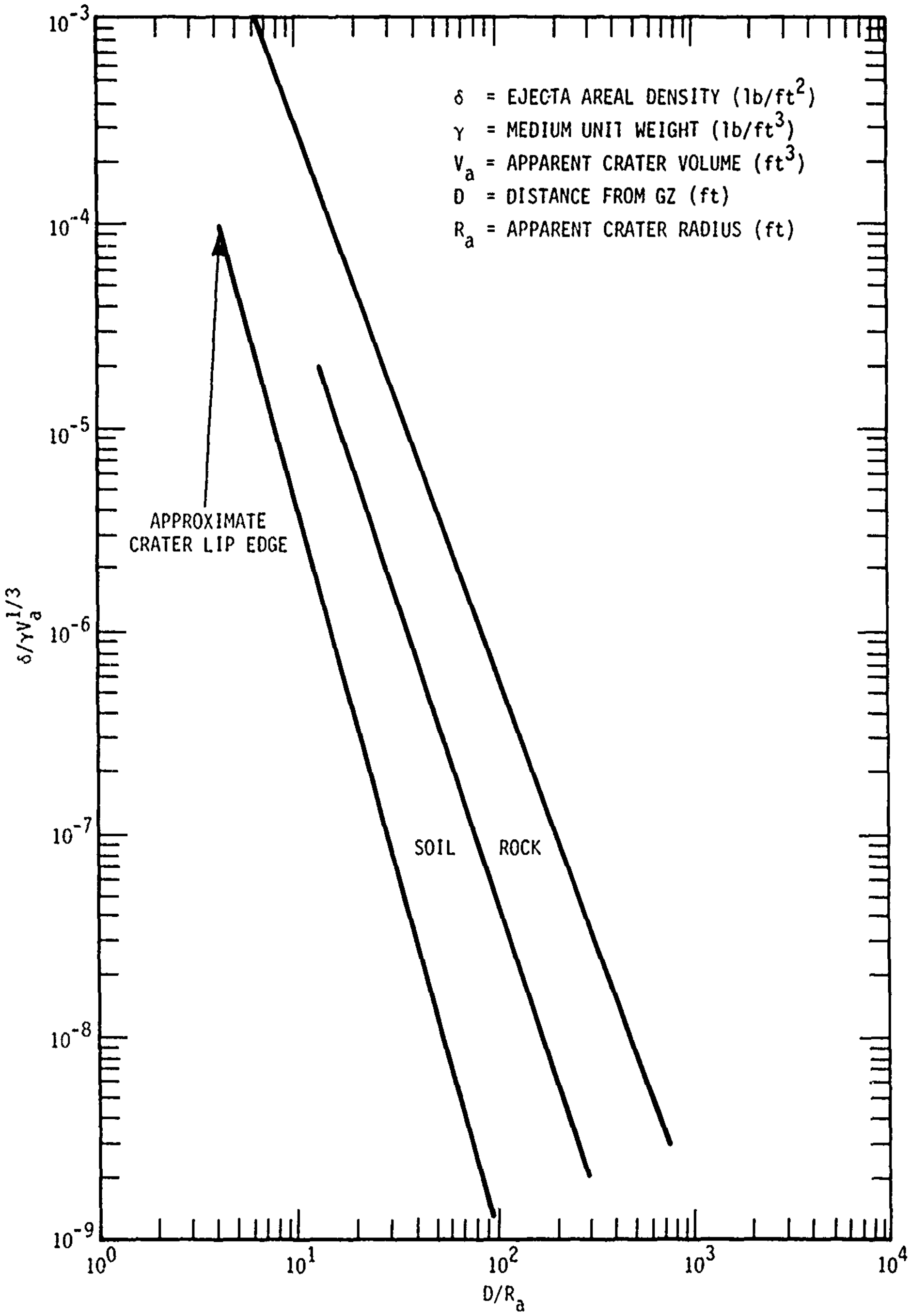

Figure 2-13. Dimensionless plot of ejecta mass density as a function of range (expressed as multiples of the apparent crater radius). (Source: Reference 10)

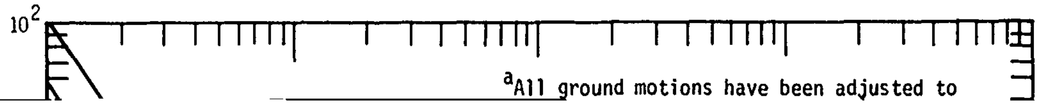

[a]All ground motions have been adjusted to

where

V_{max} = resultant peak particle velocity (cm/sec)

D = distance (m)

W = TNT-equivalent weight (tons).

Equation 2-6 is shown on Figure 2-14 for comparison with the data. Recent large field test explosions tend to confirm that Equation 2-6 is a reasonably conservative assumption for distant ground motion from near-surface explosions. Ground motions at two dams and a large tunnel were measured during the execution of Event I of MISERS BLUFF, a 120-ton charge of ANFO. The peak ground motion at one of the dams was about an order of magnitude below that predicted by Equation 2-6 and ground motions at the other dam and the tunnel were not measurable (Reference 16). Ground motion measurements for PRE-DICE THROW I, PRE-DICE THROW II, and DICE THROW generally appear to be about equivalent to, or less than, the values that would be obtained from Equation 2-6 (Reference 17).

Scaling ground motions by crater volume and comparing buried explosions with those at zero height-of-burst indicates that buried explosions produce ground shocks of approximately 4 times the magnitude determined from Equation 2-6 (Reference 18), although that analysis is only for relatively large ground motions. Since this would be a conservative estimate of the buried explosions shown in Figure 2-14, it will be assumed in this study that Equation 2-6 multiplied by 4 applies to deeply buried explosions.

Ground motion damage criteria are usually given as functions of accelerations rather than velocities. Based on MIXED COMPANY III results (Reference 11), velocities correspond to simple harmonic motion of a fundamental Raleigh wave frequency of 6 hertz, i.e., multiply V_{max} by 37.7 to obtain the value of peak acceleration. Accelerations based on Equation 2-6 are plotted on Figure 2-15 for TNT-equivalent explosive weights of interest.

EXPLOSIVE PRODUCTS

The explosion of a charge of HE results in a hot fireball of numerous chemical elements and compounds that are mostly in the gaseous state. Because of oxidation of the initial chemical products, the total weight of the final products is greater than the weight of the explosive charge. For any particular explosive, the types and amounts of chemical species can be calculated by computer programs; the problem is in determining the best values for the input parameters to the particular equation of state. Comparing computer program theoretical calculations against empirical data is extremely difficult because laboratory tests are limited to very small amounts of explosives exploded in a relatively small chamber. Under such

ethane[b]
.1
.792
-
.0
.37
.0557
-
-
.9
-
.74
-
-
-
-
.00

e-
me
tion
tion

included in the calculations from Reference 19. There is disagreement on the significance of such conditions.

Because of the large ratio of volume to surface area for a multiton explosive charge, atmospheric oxygen may not be available to a large part of the explosive products until the temperature has decreased (because of expansion of the fireball) to where significant chemical reactions will not occur. Reference 19 states that reaction rates involving oxygen are sufficiently slow that the explosion products may be "frozen" at roughly their initial proportions as they expand and cool. In contrast, the informal opinion of Dr. Harold Ring, Assistant Director of Dupont De Nemours Research Section on explosives at Wilmington, Delaware, was that equation-of-state computations do not apply for large charges exploded in the open because virtually all of the explosion products will change to water, carbon dioxide, and nitrogen.

In either event, oxidation of the compounds shown in Table 2-4 will generally tend to change potentially hazardous compounds to less hazardous or innocuous products. Therefore, Table 2-4 can be assumed as a worst-case from the standpoint of hazardous explosion products.

CLOUD RISE AND DIFFUSION

The heat of explosion creates a buoyant fireball of hot gases and earth materials which rises rapidly until it loses buoyancy, continues to expand turbulently until it reaches stabilization dimensions, and then undergoes atmospheric diffusion as it drifts downwind. According to Church (Reference 22), explosion clouds cease to rise buoyantly within about 2 minutes after detonation, although cloud growth by turbulence may give the appearance that the cloud is still rising. Based on measurements of clouds from 22 HE charges exploded on the ground surface, Church recommends that the maximum height of the cloud at 2 minutes be calculated from the empirical relationship:

$$C_t = 508\ W^{0.25} \tag{2-7}$$

where

C_t = cloud-top height at 2 minutes after detonation (m)

W = explosive charge TNT-equivalent weight (tons).

Based on Equation 2-7, a 500-ton event would have a cloud height of 2,400 meters. However, Equation 2-7 is based on few charges in excess of 1 ton and does not give information on the cloud dimensions after turbulence ceases. There is evidence that the top of the cloud produced from a large explosion continues to rise after 2 minutes, either from buoyancy or from turbulence, to reach a considerably greater height.

Figure 2-16 shows the cloud-top heights from four 500-ton explosions for which cloud measurements were made. The estimated height of a 100-ton explosion cloud is also shown. As can be seen, although Equation 2-7 adequately describes cloud height 2 minutes after an explosion, cloud heights continued to increase until about 5 minutes. From this data, it appears that the maximum cloud height for a 500 ton explosion is somewhat in excess

When a cloud reaches its maximum height, it has roughly a cylindrical shape. Most clouds appear to have a bottom that is about midway between

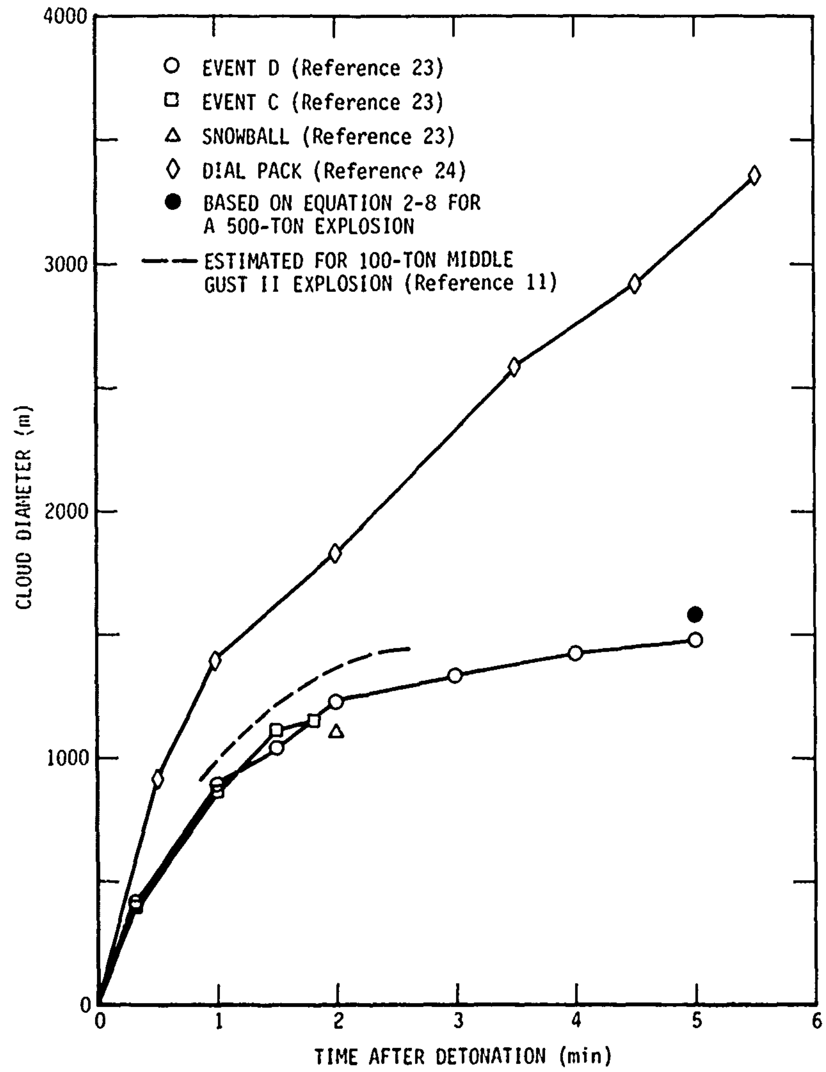

Figure 2-17. Diameters of large-explosion clouds.

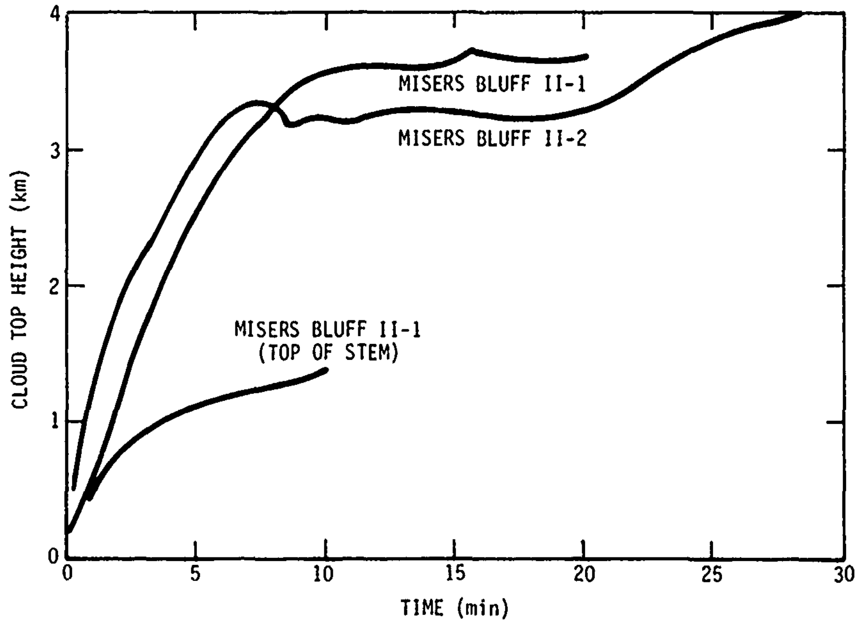

Figure 2-18. Top of MISERS BLUFF clouds. (Source: Reference 27)

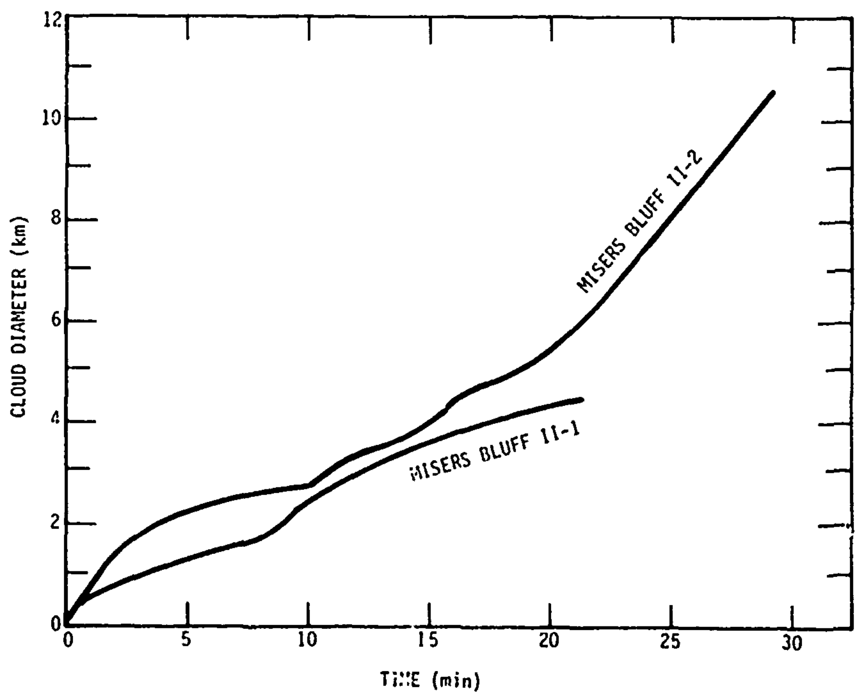

Figure 2-19. Diameter of MISERS BLUFF clouds.
(Source: Reference 27)

The cloud dimensions during the first 6 minutes are in good agreement with the other data clouds in Figures 2-16 and 2-17 and with Equations 2-8 through 2-12. The measurements of the bottom of the MISERS BLUFF II-2 cloud (the stem height) support the previous observations that the bottom of a cloud is about midway between the top of the cloud and the ground. Note, however, that the MISERS BLUFF observations were carried out over a longer time period than for the previous field tests, and they indicate that maximum cloud size at stabilization occurs later than 5 minutes after the explosion. This indicates that Equations 2-8 through 2-12 may underestimate the size of an explosion cloud at stabilization. For the purposes of environmental analysis, however, underestimation of an explosion cloud is conservative because a larger cloud is necessarily more diffuse and the concentrations of gaseous detonation products and dust at ground level downwind would be less than for a smaller cloud size at stabilization. Therefore, Equations 2-8 through 2-12 are still recommended for the purposes of environmental analysis, until more cloud measurements from other large-scale field tests are available to better estimate stabilized cloud dimensions.

Most of the earth materials from a crater fall back to earth in the vicinity of the crater. The earth materials in a stabilized cloud are relatively fine particles that can be transported downwind with the gaseous detonation products. Dust samples taken from the DIAL PACK cloud by aircraft fly-throughs showed that the average dust concentration at the time the cloud stabilized (approximately 15 minutes after the explosion) was approximately 4 mg/m^3 and the concentration decreased inversely with time to the 1.4 power over the measurement period of from 10 to 60 minutes following the explosion; that is, for each ten-fold increase in time, the dust concentration decreased by a factor of 25 (Reference 28). Based on the approximate cloud dimensions at 5 minutes of a vertical thickness of 1,500 meters and a horizontal diameter of about 3,100 meters and the apparent crater volume of 7,400 m^3, approximately 2 percent of the crater volume was in the DIAL PACK explosion cloud at the time of cloud stabilization.

The more extensive sampling and analysis of the dust clouds from MISERS BLUFF II-1 and II-2 events (Reference 29) indicate much higher concentrations than the data from DIAL PACK. Figures 2-20 and 2-21 show the cloud dimensions and concentrations from the MISERS BLUFF events at 10 and 20 minutes after the detonations, as reconstructed from the extensive data. These dust concentrations are one to two orders of magnitude greater than the concentration of the DIAL PACK cloud. The total mass of dust in the II-1 cloud 10 to 20 minutes after detonation is reconstructed to be approximately 8×10^8 grams (880 tons), which indicates approximately one-third of the crater volume of 150 m^3 was in the stabilized explosion cloud. The total mass in the multiburst II-2 cloud 10 to 20 minutes after detonation was reconstructed to be approximately 5×10^9 grams, which also indicates approximately one-third of the crater volume of 10,600 m^3 was in the stabilized explosion cloud.

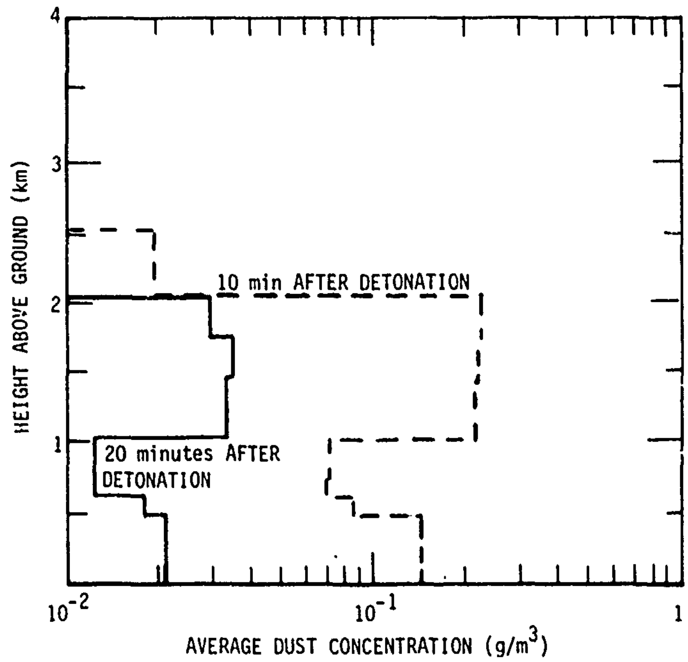

Figure 2-20. Reconstructed MISERS BLUFF II-1 dust cloud. (Source: Reference 29)

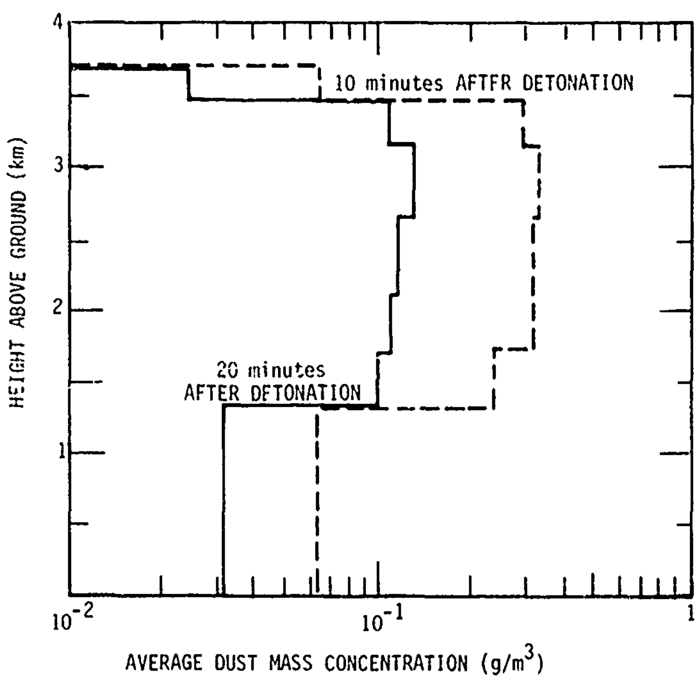

Figure 2-21. Reconstructed MISERS BLUFF II-2 (multiburst) dust cloud. (Source: Reference 29)

The sampling data from the individual aircraft sampling passes through the cloud and the cloud reconstruction indicate that, although the concentrations varied at different points in the cloud, there was no indication of the concentrations being greater at the center of the cloud. It can be assumed that the dust mass is distributed evenly throughout the cloud at the time of stabilization.

Since the recent MISERS BLUFF data are based on an extensive experimental program and are more conservative from an environmental impact standpoint than the DIAL PACK results, the results from MISERS BLUFF will be assumed in this analysis, i.e., it is assumed that one-third of the apparent crater contents will be distributed evenly throughout an explosion cloud and available for distant transport downwind as the cloud diffuses. Cloud sampling in future field tests may clarify the considerable disparity between the MISERS BLUFF and DIAL PACK data.

As an explosion cloud drifts downwind, it diffuses and the concentrations of dust and explosive products decrease while the edge of the cloud approaches ground level. At a certain distance downwind, which is a function of the initial height and dimensions of the cloud, the rates of diffusion in the horizontal and vertical directions, and wind speed, the exposure at ground level from this cloud will reach a maximum; at closer distances, the cloud has not diffused to ground level and at greater distances, the horizontal diffusion dominates to reduce the exposure below the maximum. The estimated exposure at ground level directly downwind from an explosion cloud can be calculated from Equation 2-13 which has been adapted from Reference 30:

$$E = \frac{\sigma_{XI}\,\sigma_{YI}\,\sigma_{ZI}}{\sigma_{XI}\,\sigma_{YI}\,\sigma_{ZI} + V_I} \times \frac{Q}{\pi\,\sigma_{YI}\,\sigma_{ZI}\,\bar{u}} \exp\left\{\frac{-h^2}{2\,\sigma_{ZI}^2}\right\} \tag{2-13}$$

where

E = exposure ($g \cdot sec/m^3$)

σ_{XI} = standard deviation of the distribution of material in the cloud in the horizontal downwind direction (m)

σ_{YI} = standard deviation of the distribution of material in the cloud in the horizontal crosswind direction (m)

σ_{ZI} = standard deviation of the distribution of material in the cloud in the vertical direction (m)

V_I = volume of the initial cloud, i.e., at stabilization (m^3)

Q = total mass of the material of concern in the cloud (gm)

$\bar{u}$ = average wind speed (m/sec)

h = height of point of release, i.e., height to center of the initial cloud (m).

The standard deviations in Equation 2-13 are functions of the meteorological conditions and the distance of travel of the cloud. An unstable atmosphere has a relatively large amount of vertical mixing. Such a condition results in relatively high ground level concentrations downwind and also is less likely to duct airblast. Therefore, an unstable atmosphere is not only a conservative assumption from an air pollution standpoint but is also the most likely condition when detonating a large charge of explosive.

Figure 2-22 shows recommended values of the standard deviations for cloud diffusion in an unstable atmosphere for instantaneous puffs, such as explosion clouds. Based on these values and the values for cloud height

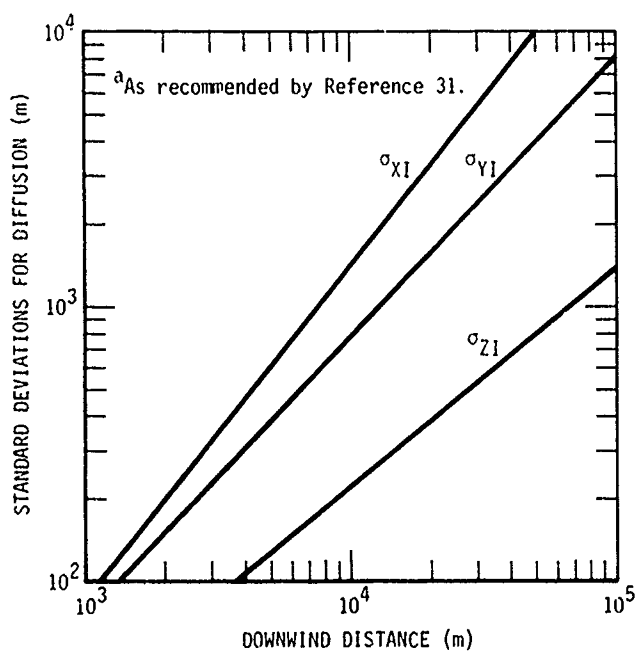

Figure 2-22. Standard deviations for diffusion parameters of instantaneous puff in unstable atmosphere.[a]

(from Equation 2-10) and for initial cloud volume (Equation 2-12), normalized calculations of exposure are shown in Figure 2-23 for some charge sizes of interest.

When the maximum values from Figure 2-23 are plotted against the TNT-equivalent weight of the explosive charge on log-log graph paper, they form straight lines, as shown in Figure 2-24. As this useful figure indicates, the maximum normalized ground level exposure (i.e., the ground level exposure for a unit mass of material in the cloud and a 1-m/sec wind) decreases with increasing charge size and occurs further downwind. The actual maximum exposure depends on the initial amount of material of interest in the cloud, the wind speed assumed, and the exposure time interval chosen.

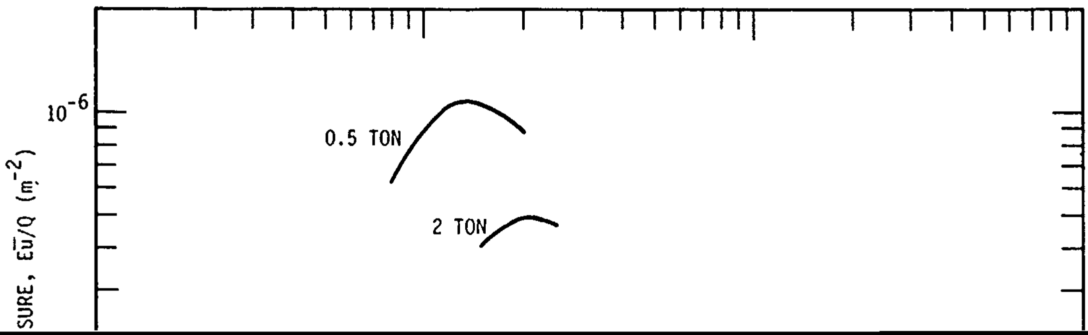

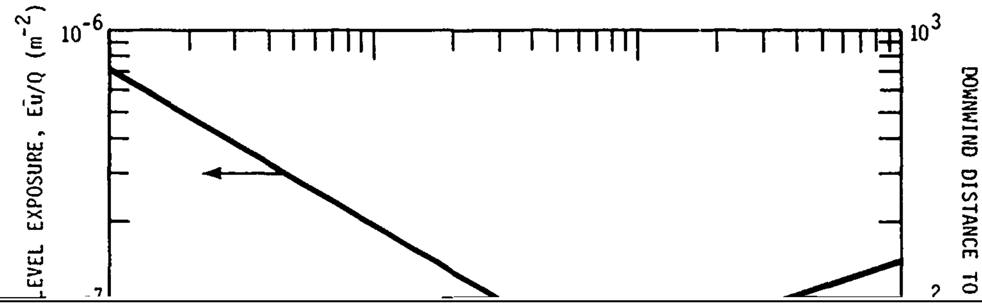

EVEL EXPOSURE, $E\bar{u}/Q$ (m^{-2})
10^{-6}
10^{3}
DOWNWIND DISTANCE TO

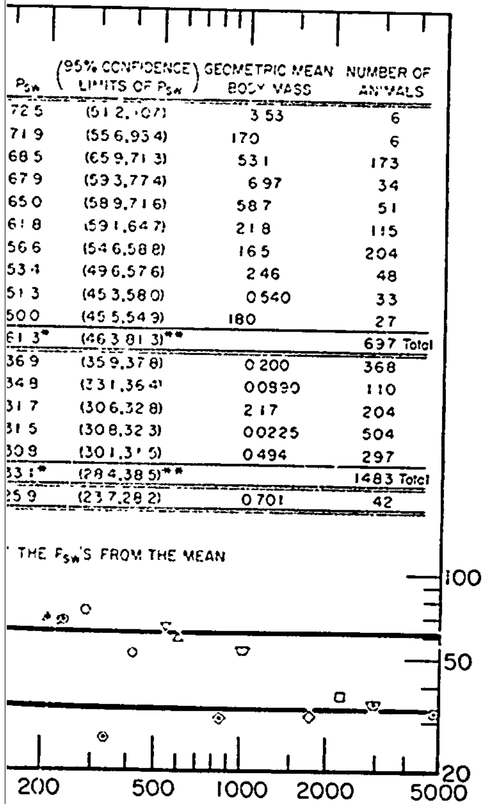

P_{sw}	(95% CONFIDENCE LIMITS OF P_{sw})	GEOMETRIC MEAN BODY MASS	NUMBER OF ANIMALS
72 5	(51 2, 107)	3 53	6
71 9	(55 6,93 4)	170	6
68 5	(65 9,71 3)	5 3 1	173
67 9	(59 3,77 4)	6 97	34
65 0	(58 9,71 6)	58 7	5 1
61 8	(59 1,64 7)	21 8	115
56 6	(54 6,58 8)	16 5	204
53 4	(49 6,57 6)	2 46	48
51 3	(45 3,58 0)	0 540	33
50 0	(45 5,54 9)	180	27
61 3*	(46 3 81 3)**		697 Total
36 9	(35 9,37 8)	0 200	368
34 8	(33 1,36 4)	00890	110
31 7	(30 6,32 8)	2 17	204
31 5	(30 8,32 3)	00225	504
30 9	(30 1,31 5)	0 494	297
33 1*	(28 4,38 5)**		1483 Total
25 9	(23 7,28 2)	0 701	42

THE P_{sw}'S FROM THE MEAN

:C

durations for "sharp-rising"
y. (The curves are computed
al.) (Source: Reference 32)

the primary mechanism of airblast damage is by tumbling or by being impacted with missiles propelled by the blast.

The 50-percent probability of lethality to small animals occurs with impacts on hard surfaces at velocities of approximately 30 to 45 ft/sec (Reference 36). (The 50-percent lethality values for these experiments were 39.4 ft/sec for mice, 43.5 ft/sec for rats, 31 ft/sec for guinea pigs, and 31.7 ft/sec for rabbits.) Statistical analysis indicated the 1-percent mortality level from impact occurs at velocities of 25 to 32 ft/sec. Based on analysis of suicide attempts by humans jumping from heights, the 50-percent lethality for humans is estimated to occur at impact velocities of approximately 54 ft/sec, and the 1-percent mortality is estimated to occur at impact velocities of roughly 20 ft/sec, with the mortalities of large animals, such as pigs and dogs, occurring at higher impact velocities (Reference 37). Experiments with dogs indicated 50-percent lethality at impact velocities of 64 ft/sec (Reference 37).

Potentially lethal velocities can be related to airblast overpressure through the acceleration coefficient of the animal. The acceleration coefficient is related to the total weight of the animal, with heavier animals having lower acceleration coefficients. References 38 and 39 give broadside acceleration coefficients for mice, rats, guinea pigs, and rabbits of approximately 0.4, 0.2, 0.15, and 0.08 ft^2/lb, respectively. For a 50-pound, four-legged animal, extrapolation of the small animal data indicates an acceleration coefficient of approximately 0.04 ft^2/lb when facing the blast and approximately 0.02 ft^2/lb when sideways to the blast.

Reference 40 relates acceleration coefficients and maximum velocities to peak overpressures from a 500-ton HE burst on the ground surface. Table 3-1 summarizes the above information and indicates that 1-percent lethality due to impact against hard surfaces can be expected for overpressures varying from about 20 kPa for a small animal such as a mouse to greater than 55 kPa for a 50-pound animal, and 50-percent lethality can be expected for overpressures varying from 28 kPa for a mouse to greater than 140 kPa for a 50-pound animal. For a man facing the blast, 1-percent and 50-percent lethality occur at peak overpressures of 50 and 110 kPa, respectively. The experimental results for birds, summarized in Figure 3-2, indicate that the threshold of injury for birds impacting against a hard surface occurs for weights of TNT that correspond to peak overpressures of approximately 14 kPa.

Summarizing Table 3-1, at distances where peak overpressure is less than 20 kPa (3 psi), few--if any--animals should be killed by translation and impact due to airblast. At distances where peak overpressures vary from 20 to 40 kPa (3 to 6 psi), some of the small animals in the open can be expected to be killed by translation and impact. At closer distances, fatalities of any larger animals can occur, with the probability of fatality increasing rapidly at distances where the peak overpressure is greater than 70 kPa (10 psi).

ɔact

Distance from 500-ton Yield (m)
520
425
460
365
<215
140
240

lds.

Small stones and other objects that are picked up by the airblast can be propelled at sufficient velocities to injure or kill animals they strike. However, the range at which injuries due to airblast-translated missiles (not missiles propelled from the crater, which are discussed elsewhere) can occur is generally within the lethal range of translation and impact by airblast. For example, a 4-ounce stone with a typical acceleration coefficient of 0.07 ft/sec^2 (Reference 38) can be picked up and achieve a peak velocity of 25 to 30 ft/sec during translation (which is the threshold of lethality due to tumbling and impact) at distances where the airblast peak overpressure is roughly 50 kPa. However, it is likely that a higher velocity would be required to produce a lethal wound; for example, Reference 40 indicates that momentums greater than 100 ft-lb/sec are required to produce skull fracture in humans (e.g., 400 ft/sec for 1/4-pound objects). Reference 41 predicts approximately one skin penetration to a human behind a window exposed to 7 kPa peak overpressure, but no penetrations of the body wall are predicted for overpressures less than about 40 kPa.

In summary, the primary damage mechanism to animals on the ground and in the open can be expected to be from translation by airblast and subsequent impact. Animals in burrows and birds in flight at close ranges can be injured by direct airblast effects. Serious injury or death from airblast-induced missiles is not likely to occur beyond the distances where translation and impact is the primary damage mechanism.

Close-In Effects on Vegetation

Reference 42 summarizes the predicted effects of airblast on trees, based on theoretical and empirical data. Damage to trees, expressed as the percent of trees downed, is a function of type and class of tree, height of tree (for conifers), and type of site. Figure 3.2 summarizes the informa-

GEND.

Type	Class	Height (feet)	Site*
Broadleaf	Small leaves or light crown (birch, poplar, scarlet oak)		Poor
Broadleaf	Small leaves or light crown (birch, poplar, scarlet oak)		Good
Broadleaf	Large leaves or heavy crown (beech, maple, hickory, sycamore)		Poor
Broadleaf	Large leaves or heavy crown (beech, maple, hickory, sycamore)		Good
Broadleaf	Defoliated		Average
Conifer	Light crown (spruce, cedar, hemlock, larch)	40	Poor
Conifer	Light crown (spruce, cedar, hemlock, larch)	80	Poor
Conifer	Light crown (spruce, cedar, hemlock, larch)	120	Poor
Conifer	Light crown (spruce, cedar, hemlock, larch)	40	Good
Conifer	Light crown (spruce, cedar, hemlock, larch)	80	Good
Conifer	Light crown (spruce, cedar, hemlock, larch)	120	Good
Conifer	Heavy crown (pine, fir)	40	Poor
Conifer	Heavy crown (pine, fir)	80	Poor
Conifer	Heavy crown (pine, fir)	120	Poor
Conifer	Heavy crown (pine, fir)	40	Good
Conifer	Heavy crown (pine, fir)	80	Good
Conifer	Heavy crown (pine, fir)	120	Good

ood site has adequate rainfall, etc., which does not promote a deep root structure while poor site has lack of rain, rocks, etc., which promote a deep root structure with great holding power.

on of explosive yield and overpressure.

Close-In Effects on Structures

Field tests are usually conducted in isolated areas with few, if any, manmade structures in the nearby vicinity, except those that pertain to the test. Also, many of the structures in field test areas (e.g., utility lines, fences) lack the broad surfaces that are most vulnerable at relatively low peak overpressures; such types of structures are typically not damaged by overpressures less than at least several tens of kPa from a large HE burst. Glasstone (Reference 43) shows damage/distance relationships for various types of structures exposed to nuclear explosions. These nomographs indicate that wood-frame buildings typically are badly damaged

In summary, the structural integrity of most structures is not threatened by overpressures less than 10 kPa. At higher overpressures, damage to most types of buildings increases rapidly. Seven kPa is about the threshold of failure for light exterior walls and interior partitions of buildings. Below 7 kPa, damage is limited to sensitive features of buildings such as windows and plaster.

Explosives Safety Standards

Department of Defense (DOD) Directive 5154.4S, DOD Ammunition and Ex-

EFFECTS ON STRUCTURES. Window glass failure can occur at a lower overpressure level than any other type of structural material. An earlier Bureau of Mines report, based on small-charge data, recommended a "safe" airblast overpressure level of 0.5 psi (3.5 kPa) (Reference 47). Nuclear

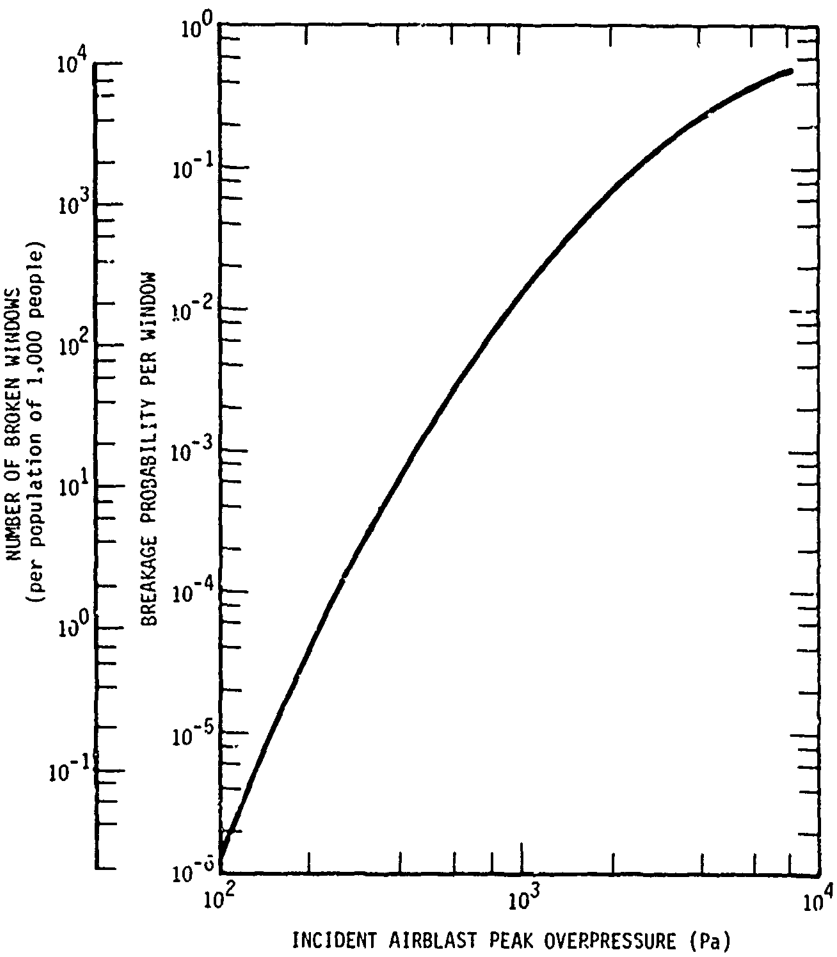

Figure 3-4. Window damage as a function of airblast overpressure. (Based on Reference 1)

The best estimate of the number of window panes per capita in an urban area is an average of 19 panes per person, based on a survey of San Antonio, Texas, in 1963 following an accidental explosion of 57 tons of HE at the Median Base which broke over 3,000 windows in the city. Based on this estimate, the extreme left-hand scale of Figure 3-4 estimates the number of broken windows (per human population of 1,000) that can be expected in a population center at any given magnitude of incident airblast peak overpressure. An overpressure of a few hundred Pa can cause a very large amount of window damage in urban and suburban areas, which may have population densities of thousands or tens of thousands of people per square mile.

Quantitative data on distant airblast magnitudes that can damage historic buildings, archaeological features, and significant natural physical features or that could cause rock or snow slides are sparse. Most such information comes from sonic boom experiments and analyses and is summarized in References 51 and 54. The consensus is that the nominal sonic boom peak overpressure magnitude of 100 to 200 Pa is only one of the sources of vibration that contributes to the "ageing" of a structure (or a natural feature) to the point where damage might occur.

As shown in Section 2, airblast in excess of 100- to 200-Pa peak overpressure can occur over very large areas, hundreds or thousands of square miles of area in the case of a large-yield explosion. Lower overpressures are comparable with close thunder (135 dB or 100 Pa) (Reference 55). While adverse effects were observed in humans exposed to a series of extremely high-level sonic booms (3 to 7 kPa, or up to 1 psi) (Reference 59). Although hearing acuity was not physically measured, the subjects reported no indication of any observable symptoms of hearing loss or other ear involvement. In this same experiment, no significant adverse effects on livestock were observed.

In summary, there is no firm evidence to indicate that occasional impulse sounds below the level that will produce physical damage to living organisms produce any lasting significant adverse effects.

NOISE STANDARDS. The Environmental Protection Agency (EPA) has judged that exposure to less than 145-dB (0.05-psi or 350-Pa) impulse noise no more than once per day is "acceptable" in that hearing damage will not result (Reference 60). The occupational limit for industrial workers is 140 dB (0.03 psi or 200 Pa) (Reference 61). These noise levels can be exceeded many miles away from a large-yield explosion.

Technically, distant blast noise qualifies as impulse noise because neither References 60 nor 61 make any allowance for rise time or frequency spectrum of the impulse. However, noise from distant explosions is predominantly low frequency, mostly below 10 Hz, against which the ear strongly discriminates. On the A-weighted scale, which approximates the relative response of the human ear to frequencies, the ear discriminates against a frequency of 10 Hz by about 70 dB. In other words, a 10-Hz frequency having a sound pressure level of 145 dB would be perceived by a listener as having a magnitude of approximately 70 dB less, i.e., 75 dB. Distant airblast may therefore have an unweighted sound pressure level that exceeds recommended limits of 140 or 145 dB, but which is of such low frequency that the ear discriminates against it to the extent that the noise level is not greatly disturbing to the average person and may not be perceived by some people. (Annoyance from low-frequency shock waves is often related to rattling of windows and other building components, rather than hearing the shock wave directly.)

The recommended limit of 145 dB to the general public is not a law. The Occupational Safety and Health Administration (OSHA) limit of 140 dB presumably applies to personnel at test sites, but was designed for industrial conditions where hearing loss can occur to workers repeatedly exposed to impulsive noise. Carried to the extreme, many actions involve noise levels that exceed the OSHA limit. For perspective, the ear of a person firing a handgun is exposed to sound pressure levels of from 140 to 170 dB, or nearly 7 kPa (Reference 60).

Damage Distances

Table 3-2 summarizes threshold levels for damage from airblast. In Figures 3-5 and 3-6, levels are overlaid on the graphs of airblast peak overpressures versus distance that were developed in Section 2 to

Table 3-2. Summary of airblast damage threshold levels.

Effect	Corresponding Incident Peak Overpressure Level
Threshold of lethality	
Small animals in the open	20 - 40 kPa
50-pound animal in the open	>55 kPa
Small animals (rabbits or smaller) in burrows	190 kPa[a]
Larger animals in burrows	320 kPa[a]
Threshold of lung damage to animals in burrows	
Small animals	45 kPa[a]
Large animals	85 kPa[a]
Threshold of eardrum rupture to animals in the open	20 - 35 kPa
Threshold of injury to birds in flight	35 - 70 kPa
Toppling of trees (small leaves or defoliated or light crowned)	35 - 70 kPa
Damage to small vegetation or tree branches	20 kPa
Damage to building walls/roofs	7 kPa
Skin penetrations from broken windows	3.5 kPa
Flight hazard to light aircraft	1.4 kPa
Window breakage (one window for each 1,000 of human population)	200 Pa
Impulsive noise level limit for industrial workers by Occupational Safety and Health Administration (OSHA)	140 dB (0.2 kPa)
Tinnitus or "ringing" of ears	160 dB (2 kPa)

[a]The peak overpressure levels shown are the levels that occur without reflections. Airblast filling a burrow can produce pressures that are 2 to 3 times these values and are sufficient to result in the effect that is described.

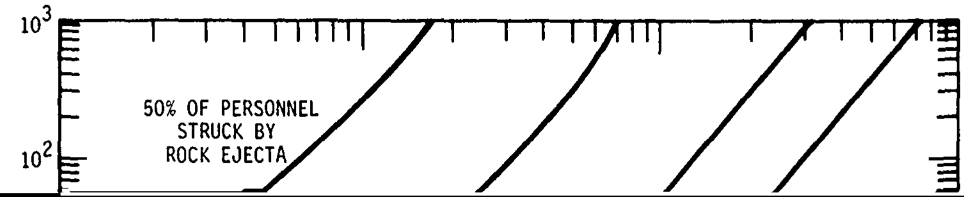
10^3
10^2
50% OF PERSONNEL
STRUCK BY
ROCK EJECTA

Table 3-3. Modified Mercalli Intensity Scale of 1931 (abridged).[a]

I.	Not felt except by a very few under especially favorable circumstances. (I Rossi-Forel Scale)
II.	Felt only by a few persons at rest, especially on upper floors of buildings. Delicately suspended objects may swing. (I to III Rossi-Forel Scale)
III.	Felt quite noticeably indoors, especially on upper floors of buildings, but many people do not recognize it as an earthquake. Standing motorcars may rock slightly. Vibration like passing truck. Duration estimated. (III Rossi-Forel Scale)
IV.	During the day, felt indoors by many; outdoors by few. At night, some awakened. Dishes, windows, and doors disturbed; walls make creaking sound. Sensation like heavy truck striking building. Standing motorcars rocked noticeably. (IV to V Rossi-Forel Scale)
V.	Felt by nearly everyone; many awakened. Some dishes, windows, etc. broken; a few instances of cracked plaster; unstable objects overturned. Disturbance of trees, poles, and other tall objects sometimes noticed. Pendulum clocks may stop. (V to VI Rossi-Forel Scale)
VI.	Felt by all; many frightened and run outdoors. Some heavy furniture moved; a few instances of fallen plaster or damaged chimneys. Damage slight. (VI to VII Rossi-Forel Scale)
VII.	Everybody runs outdoors. Damage negligible in buildings of good design and construction; slight to moderate in well-built ordinary structures; considerable in poorly-built or badly-designed structures. Some chimneys broken. Noticed by persons driving motorcars. (VIII Rossi-Forel Scale)
VIII.	Damage slight in specially-designed structures; considerable in ordinary substantial buildings, with partial collapse; great in poorly-built structures. Panel walls thrown out of frame structures. Fall of chimneys, factory stacks, columns, monuments, walls. Heavy furniture overturned. Sand and mud ejected in small amounts. Changes in well water. Persons driving motorcars disturbed. (VII+ to IX Rossi-Forel Scale)
IX.	Damage considerable in specially-designed structures; well-designed frame structures thrown out of plumb; great in substantial buildings, with partial collapse. Buildings shifted off foundations. Ground cracked conspicuously. Underground pipes broken. (IX+ Rossi-Forel Scale)
X.	Some well-built wooden structures destroyed; most masonry and frame structures destroyed with foundations; ground badly cracked. Rails bent. Landslides considerable from river banks and steep slopes. Shifted sand and mud. Water splashed (slopped) over banks. (X Rossi-Forel Scale)
XI.	Few, if any, structures (masonry) remain standing. Bridges destroyed. Broad fissures in ground. Underground pipelines completely out of service. Earth slumps and land slips in soft ground. Rails bent greatly.
XII.	Damage total. Waves seen on ground surfaces. Lines of sight and level distorted. Objects thrown upward into the air.

[a]Harry O. Wood and Frank Neuman, in Bulletin of the Seismological Society of America, Vol. 21, No. 4, December 1931.

$$I_{MM} = \log 14v/\log 2 \quad (3\text{-}4)$$

$$\log a = 0.25\ I_{MM} + 0.25 \quad (3\text{-}5)$$

where

- a = peak particle acceleration in cm/sec^2 (except in Equation 3-5, it is the peak horizontal component)
- v = peak particle velocity in cm/sec
- I_{MM} = Modified Mercalli Scale values.

Based on Equations 3-3 through 3-5, earthquake-induced ground motion velocities of approximately 2 to 4 cm/sec and accelerations of 15 to 30 cm/sec^2 correspond to an I_{MM} value of V, the threshold of slight architectural damage.* One can be confident that ground motions of these magnitudes caused by chemical explosions will not cause significant damage because of their relatively short duration and higher frequency, compared to earthquakes.

INITIATION FROM EXPLOSIONS. There has been concern as to whether un

Based upon Reference 67, 600 tons of TNT buried and exploded in alluvium has a seismic magnitude of approximately 2.5. Experience with earthquakes in California indicates that a typical earthquake of this magnitude would be barely felt and would produce I_{MM} intensities of less than III at the epicenter (Reference 62), intensities that are not damaging to even the most sensitive manmade structures. Thus, initiation of a significant earthquake by a chemical explosion does not seem to be a credible possibility.

Effects on Buildings

Based on the results of a 10-year program to determine ground vibrations from blasting and their effects on structures, the U.S. Bureau of Mines established a criterion of 5 cm/sec for peak particle velocity ground motions to ensure no damage to residences (Reference 68). Vibrations from blasting cannot exceed a velocity vector magnitude of 5 cm/sec at any point in the ground near the foundation of a residence. As cited in Reference 68, earlier studies indicated that fine plaster cracks began to occur at ground motions from blasting of from 5 to 10 cm/sec.

Examination of Soviet Union blasting criteria in Table 3-4 indicates general agreement with the U.S. Bureau of Mines criterion for residences. In general, then, a safe blasting criterion to buildings and other structures is 3- to 5-cm/sec peak ground motion velocities, except perhaps for "large-panel buildings" where a criterion of 1.5 cm/sec is recommended based on Soviet experience. These criteria for transient ground motions from blasting are consistent with recommended limits to rotating machinery and machinery foundations of 2.5 cm/sec at steady-state frequencies below approximately 2,000 rpm (Reference 69).

These ground motion criteria of 1.5 to 5 cm/sec, or less, to assure no damage to buildings are met beyond relatively close distances from HE field tests, where damage from airblast predominates. For example, these criteria were met at distances beyond 700 to 1,500 meters from the 500-ton MIXED COMPANY III field test where the airblast peak overpressures of 14 to 5 kPa would have caused significant damage to buildings.

Initial experience with nuclear weapons testing seemed to indicate that a threshold for producing small cracks in plaster was approximately 20 cm/sec for newly-constructed residences and 10 cm/sec for older residences (References 70 and 71). The prevailing concept of a nuclear damage threshold between 5 and 10 cm/sec to structures, in conformance with experience from blasting with HE, was "rudely shattered" in 1964 by the SALMON nuclear test, a 5-KT underground test, when valid damage claims were received where it was certain that the ground motions were less than 5 cm/sec (Reference 72).

It now appears that there were at least three reasons why the SALMON nuclear test produced damage at considerably lower ground motion magnitudes than was expected, based on experience with HE and limited nuclear blast

Table 3-5. Ground motion measurements near RULISON nuclear underground test. (Source: Reference 74)

Location	Slant Range (km)	Peak Vector Ground Motion: Acceleration (cm/sec^2)	Velocity (cm/sec)	Displacement (cm)
Grand Valley	10.6	540	8.27	0.236
Rifle				
Union Carbide	18.0	170	3.57	0.139
Church	20.2	94	3.13	0.106
Top of Hill	20.2	135	3.77	0.410
De Beque				
Station No. 1	22.8	100	2.20	0.099
Station No. 2	22.8	159	4.68	0.206
Collbran	18.8			
Silt (radial	29.8	33	1.34	0.068

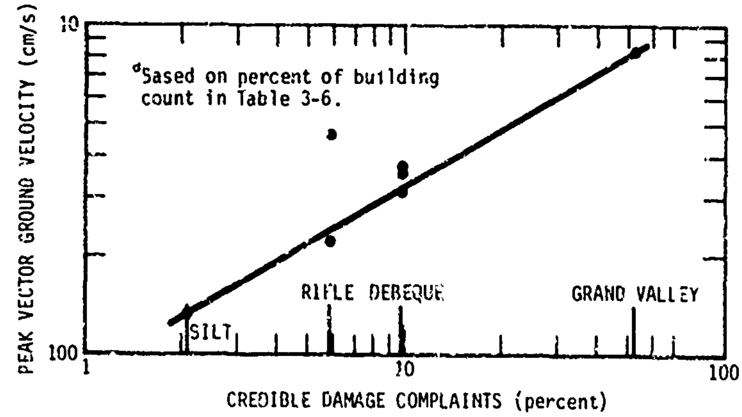

Figure 3-8. Credible damage complaints versus peak vector ground velocity.[a] (Source: Reference 74)

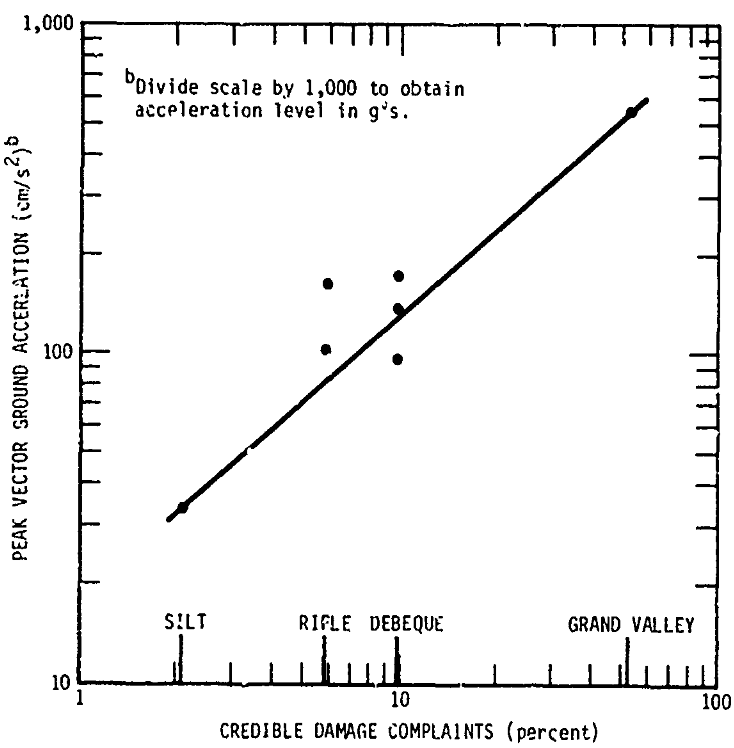

Reference 71 does not give a threshold criterion for steel storage tanks but predicts severe damage to tanks of light construction at ground motions of 80 cm/sec. There was no damage to 10 small privately-owned water and fuel tanks located within 8 kilometers of the GNOME event, a 3-KT nuclear explosion fully contained in salt (Reference 71).

The threshold of structural damage to rigid-frame prefabricated buildings is in excess of 150 cm/sec, while the threshold of structural damage to small plywood buildings is 150 cm/sec (Reference 71). Instrumentated trailer vans on styrofoam pads have a damage threshold in excess of 300 cm/sec, while some types of light-wheeled heavily-loaded trailers suffer severe damage at 100 cm/sec. Other types are undamaged at greater ground motions (Reference 71). At 30 cm/sec, light objects can be thrown about (Reference 71).

A large number of 25-foot wooden utility poles erected in concrete bases at GZ of the GNOME event were undamaged (Reference 70). Two old 8-inch-diameter, guyed, 50-foot steel towers located approximately 300 meters from GZ of the BILBY event (a 200-KT fully-contained nuclear explo-depth is typically not quite double the apparent crater depth; therefore, the vertical fracture zone for rock is approximately 6 times the apparent crater depth and the vertical displacement zone is approximately 8 times the apparent crater depth. Based on Equations 2-3 and 2-5 (see Section 2), the vertical limit for fracturing of rock (assuming a zero height-of-burst) would thus vary from about 8 meters for a 1-ton explosion to about 60 meters for a 500-ton explosion and the corresponding limits of displacement would be from about 10 and 75 meters, respectively. These values can be assumed as maximum limits for damage to bedrock beneath a layer of soil (unless the charge is significantly buried) because the soil layer will attenuate the shock to a greater extent than if the medium were entirely rock. In summary, if bedrock is at a lesser depth below the ground surface than indicated by the above approximate figures, the bedrock might possibly be damaged by a near-surface explosion. However, such damage has no environmental significance unless the bedrock is supporting or restraining a water table.

Effects on Animals and Humans

Reference 78 summarizes the observations of wildlife and domesticated animals exposed to ground motions from underground nuclear explosions. Physical damage to such animals has never been observed, even though the ground motions were several g's in some instances (1 g equals nearly 1,000 cm/sec^3). For example, cows and calves located near GZ of the CLEARWATER underground nuclear test suffered no physical damage at ground motions of from 2.5 to 4 g's and 140 to 230 cm/sec, although one cow was knocked to its knees. Other tests on cattle, horses, deer, and elk at lower ground motions had essentially negative results. The milk production of lactating

Table 3-7. Human response to ground motions. (Source: Reference 69)

Vibration From	Authority	Details	Observed: Amplitude (in.)	Observed: Frequency (cycles/sec)	Reiher and Meister Classification	Derived: Maximum Velocity (μin./sec)	Derived: Acceleration (g)
Traffic	Hyde and Lintern (1929)	Single-deck motor bus, 18 mph, 30 feet away	0.00012	26	Just perceptible	19,700	0.0082
Traffic	Hyde and Lintern (1929)	Light truck, 13.6 mph, 20 feet away; rough road	0.00012	20	Just perceptible	15,100	0.0049
Traffic	BRS (1934)	General traffic at Brentford	0.00012	19	Just perceptible	14,300	0.0044
Traffic	Tillman (1933)	Measurements in house 30 to 50 feet from traffic	0.00025	24	Clearly perceptible	37,700	0.0145
Traffic	BRS (1950)	Vibrations from London; traffic as measured inside a building	0.00014	25	Just perceptible	22,000	0.009
Traffic	BRS (1950)	Traffic measurements in Queens Street, London	0.00031	14	Just perceptible	27,000	0.0062
Traffic	BRS (1950)	Traffic measurements in Farrington Street, London	0.00036	10	Just perceptible	22,600	0.003
Railways	US	Measurements of vibration in Times Building (NY), subway; floor vibrations	0.00078	15-20	Clearly perceptible	85,000	0.024
Railways	Mallock (1902)	Hyde Park area; building vibrations due to subway	0.001	10-15	Clearly perceptible	78,000	0.01
Railways	C.C. Williams	Freight train at 65 feet; passenger train at 25 to 30 feet	0.0009 0.0037				
Pile Driving	BRS	Close to occupied building	0.00053	30	Clearly perceptible--annoying	100,000	0.049

(Continued)

Table 3-7. (Continued)

	Observed			Derived	
	Amplitude (in.)	Frequency (cycles/sec)	Reiher and Meister Classification	Maximum Velocity (µin./sec)	Acceleration (g)
amaged ed by	0.0015 0.00007	6 80	Clearly perceptible Clearly perceptible	57,500 36,000	0.006 0.045
100 feet nd	0.0017	9.4	Clearly perceptible--annoying	100,000	0.015
te fac- nearby	0.00056	42	Annoying	147,500	0.09
hird 20-hp	0.0008	3.5	Just perceptible	17,500	0.01
rements	0.005	25	Painful	780,000	0.32
d house raphic	0.00031	64	Annoying	125,000	0.133

the maximum velocities involved at the various stages of perceptibility are (ap-

10,000 to 30,000
30,000 to 100,000
Over 100,000

100 to 250,000 µin./sec and a faintly-perceptible-vibration of 25,000 to 63,000.

Damage Distances

In summary of the preceding discussion, it appears that a criterion of 20 cm/sec^2 (corresponding to a velocity of 0.5 cm/sec) for ground motions from large chemical explosions is a conservative criterion to ensure no significant damage. (For smaller contained explosions of a few tons, for example, the Bureau of Mines standard of 5 cm/sec for no damage is applicable.) This 20-cm/sec^2 level corresponds to a level that is annoying to humans but has only a 1-percent probability of damaging a residence, and below which rock slides have not been observed to occur. At a lower crite- [illegible]

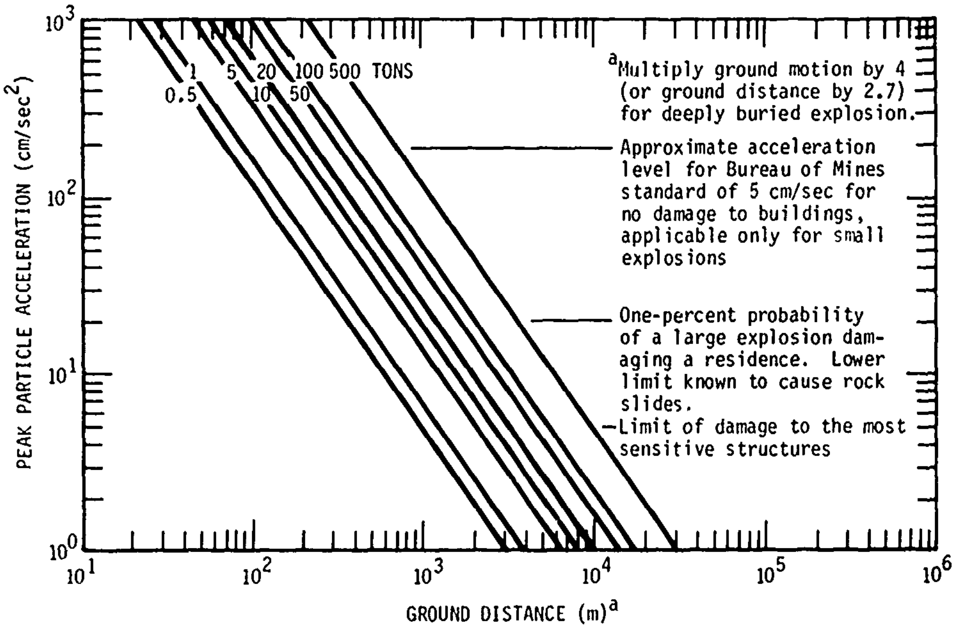

Figure 3-10. Damage-distance criteria for ground motions from near-surface explosions.

Phase II field test. The results of this program (Reference 16) indicate that ANFO explosions do not increase the salinity or cyanide concentration of soils and water. However, following the explosive tests, an increase in nitrate concentration was observed in one well that intersected the underwater flow from the crater area. The investigators concluded that the increase was probably caused by an increase in the nitrate levels in the ejecta used to fill the explosion craters; however, laboratory studies in-nitrogen-containing compounds react with secondary amines, a group of organic compounds that can be considered as derived from ammonia with two of the hydrogen atoms replaced with organic radicals. The remaining nitrogen atom in the amine links with a nitroso group (i.e., a NO radical) to form the N-nitroso compound. Since Table 2-4 indicates that several nitrogen compounds are produced by the explosion of ANFO and since secondary amines are widely distributed in the environment, it would not be surprising if nitrosamines are produced. It does not appear that the question of nitrosamines has been addressed before in the context of explosive products. Ammonium nitrate is a common fertilizer and has been used as a blasting agent for many years.

Despite being potent carcinogens, it is known that nitrosamines are widely distributed in the environment--they are formed in soil and water by the reaction of nitrogen compounds with naturally occurring amines, they are present in tobacco smoke, they are formed in the human stomach when nitrites are ingested, and they occur in human saliva. Since the vicinity of most test sites is not used for human food crops or public water supply, it does not appear that any human hazard would result in most cases even if nitrosamines are produced.

The gaseous detonation products and the fine dust in the explosion

24. Hyman, D.S., et al., Dust Cloud Analysis for Event DIAL PACK, DASA 2694, CR-1-219, prepared by General Research Corporation for Defense Atomic Support Agency (now DNA), May 1971.

25. Sprague, K.E., et al., MIDDLE COURSE II Cratering Series, Technical Report E-73-3, U.S. Army Waterways Experiment Station, Livermore, California, AD765436, July 1973.

26. Fitchett, Major D.J., MIDDLE COURSE I Cratering Series, NCG Technical Report Number 35, TID-4500, UC-35, U.S. Army Engineer Nuclear Cratering Group, Livermore, California, June 1971.

27. Boquist, W.P., "Optical Measurements of MISERS BLUFF Multiburst Cloud Phenomenology," Proceedings of the MISERS BLUFF Phase II Results Symposium, 27-29 March 1979, Volume III, DNA 5192, Defense Nuclear Agency, 26 September 1979.

28. Green, W.E., Airborne Sampling and Analysis of Particulates from the DIAL PACK Event, DASA 2600 (MR170 FR-948), Headquarters, Defense Atomic Support Agency, Washington, D.C., January 1971.

29. Thomas, C.R., and J.E. Cockayne, MISERS BLUFF Cloud Sampling Program, Data Summary and Dust Cloud Characterizations, DNA 5189F, Defense Nuclear Agency, 7 December 1979.

30. Slade, D.H., Ed, Meteorology and Atomic Energy 1968, U.S. Atomic Energy Commission, Air Resources Laboratories, Office of Information Services, July 1968.

31. Beals, Major G.A., USAF ETAC, Guide to Local Diffusion of Air Pollutants, Technical Report 214, Air Weather Service, USAF, available through DD2, AD726984, May 1971.

32. White, C.S., et al., The Biodynamics of Airblast, DNA 2738T, Lovelace Foundation for Medical Education and Research, Albuquerque, New Mexico, 1 July 1971.

33. Damon, E.G., et al., The Tolerance of Birds to Airblast, DNA 3314F, Director, Defense Nuclear Agency, Washington, D.C., July 1974.

34. Gesswein, J., and P. Carrao, The Position of Eardrum Rupture and Hearing Loss in the Scale of Injuries from Nuclear Blast, NSCDC 3789, Naval Ship Research and Development Center, Bethesda, Maryland, February 1972.

35. Richmond, D.R., et al., The Relationship between Selected Blast-Wave Parameters and the Response of Mammals Exposed to Air Blast, DASA 1860, Lovelace Foundation for Medical Education and Research, Albuquerque, New Mexico, November 1966.

36. Richmond, D.R., et al., Tertiary Blast Effects: The Effects of Impact on Mice, Rats, Guinea Pigs and Rabbits, DASA 1245, Lovelace Foundation for Medical Education and Research, Albuquerque, New Mexico, 28 February 1961.

37. TTCP Panel N-5 Meeting--21-23 March 1972, DASIAC SR-139, DASIAC, General Electric-TEMPO, Santa Barbara, California, July 1972.

38. Bowen, I.G., et al., Translational Effects of Air Blast from High Explosives, DASA 1336, Lovelace Foundation for Medical Education and Research, Albuquerque, New Mexico, 7 November 1962.

39. Fletcher, E.R., et al., Determinations of Aerodynamic-Drag Parameters of Small Irregular Objects by Means of Drop Tests, CEX-59.14, Lovelace Foundation for Medical Education and Research, Albuquerque, New Mexico, June 1960.

40. Bowen, I.G., et al., Translational Effects of Blast Waves, DA-49-146-XZ-055, Lovelace Foundation for Medical Education and Research, Albuquerque, New Mexico, 11 March 1963.

41. Richmond, D.R., et al, "Blast Biophysics; Past, Present and Future," Proceedings of the MISERS BLUFF Phase II Results Symposium, 27-29 March 1979, Volume III, POR 7013-3, Defense Nuclear Agency, 29 September 1979.

42. Morris, P.J., Forest Blowdown from Nuclear Airblast, DNA 3054F (URS 7049-10, Rev. I), URS Research Company, San Mateo, California, July 1973.

43. Glasstone, S., and P.J. Dolan, The Effects of Nuclear Weapons, U.S. Government Printing Office, Washington, D.C., 1977.

44. Pickering, E.E., and J.L. Bockholt, Probabilistic Air Blast Failure Criteria for Urban Structures, SRI Project 6300, Stanford Research Institute, Menlo Park, California, November 1971.

45. Wilton, C., and B. Gabrielsen, Summary Report: House Damage Assessment, DNA 2906F, Headquarters, Defense Nuclear Agency, Washington, D.C., January 1973.

46. Reed, J.W., Simplified Blast Nuisance Predictions for Small Explosions, Sandia Laboratories, Albuquerque, New Mexico, 9 July 1974.

47. Nicholls, H.R., C.F. Johnson, and W.I. Duvall, Blasting Vibrations and Their Effects on Structures, Bureau of Mines Bulletin 656, U.S. Department of the Interior, Washington, D.C., 1971.

48. Wiggins, J.H., Jr., "Sonic Boom Damage to Structures," Institute of Environmental Sciences, 1969 Proceedings, 15th Annual Technical Meeting--Man in His Environment, 20-24 April 1969, Anaheim, California, Institute of Environmental Sciences, Mt. Prospect, Illinois, pp 189-197.

49. Reed, J.W., Acoustic Wave Effects Project: Airblast Prediction Techniques, SC-M-69-332, Sandia Laboratories, Albuquerque, New Mexico, 1969.

50. Maglieri, D.J., V. Huckle, and T.L. Parrott, Ground Measurements of Shock-Wave Pressure for Fighter Airplanes Flying at Very Low Altitudes and Comments on Associated Response Phenomena, NASA TN-E-3443, Langley Research Center, Langley Station, Hampton, Virginia, July 1966.

51. Warren, C.H.E., "Recent Sonic-Bang Studies in the United Kingdom," Journal of the Acoustical Society of America, Vol. 51, No. 2 (Part 3): 783-788, February 1972.

52. Weber, G., "Sonic Boom Effects 11.1: Structures and Terrain," Journal of Sound and Vibration, Vol. 20, No. 4:531-534, 1972.

53. Wiggins, J.H., Jr., Effects of Sonic Boom, J.H. Wiggins Company, Palos Verdes Estates, California, 1969.

54. The Effects of Sonic Boom and Similar Impulsive Noise on Structures, NTID300.12, U.S. Environmental Protection Agency, Washington, D.C., December 31, 1971.

55. Nixon, C.W., Proceedings of Noise as a Public Hazard, ASHA #4, February 1969.

56. Cotterau, P., "Sonic Boom Exposure Effects 11.5: Effects on Animals," Journal of Sound and Vibration, Vol. 20, No. 4:531-534, 1972.

57. Civil Aircraft Sonic Boom Regulation (Final EIS), EIS-AA-73-0115-F, Federal Aviation Administration, Washington, D.C., January 1973.

58. Bell, W.B., "Animal Response to Sonic Booms," The Journal of the Acoustical Society of America, Vol. 51, No. 2 (Part 3):758-765, February 1972.

59. Nixon, E.W., H.K. Hille, H.C. Sommer, and E. Guild, Sonic Booms Resulting from Extremely Low-Altitude Supersonic Flight: Measurements and Observations on Houses, Livestock and People, AMRL-TR-68-52, Aerospace Medical Research Laboratories, Aerospace Medical Division, Air Force Systems Command, Wright-Patterson Air Force Base, Ohio, October 1968.

60. Information on Levels of Environmental Noise Requisite to Protect Public Health and Welfare with an Adequate Margin of Safety, 550/9-74-004, U.S. Environmental Protection Agency, Office of Noise Abatement and Control, U.S. Government Printing Office, Washington, D.C., March 1974.

61. "Occupational Noise Exposure," Code of Federal Regulations, Title 29, Paragraph 1910-95, pp 220-221, Rev. January 1, 1972.

62. Richter, C.F., Elementary Seismology, W.H. Freeman and Company, San

71. Cauthen, L.J., Jr., Survey of Shock Damage to Surface Facilities and Drilled Holes Resulting from Underground Nuclear Detonations, UCRL-7964, Lawrence Radiation Laboratory, University of California, Livermore, California, July 1964.

72. Holzer, F., Ground Motion Effects from Nuclear Explosions: A Review of Damage Experience and Prediction Methods, UCRL-51062 (TID-4500, UC-35), Lawrence Radiation Laboratory, University of California, Livermore, California, June 2, 1971.

73. Shamin, V.M., "Seismic Effect of Powerful Explosions," Doklady of the Academy of Sciences U.S.S.R., Earth Science Sections, Volume 135, March-April 1969, published by the American Geological Institute.

74. Structural Response Studies for Project RULISON, Report JAB-99-78,

DISTRIBUTION LIST

DEPARTMENT OF DEFENSE

Armed Forces Radiobiology Rsch Institute
ATTN: Director

Assistant to the Secy of Defense
Atomic Energy
ATTN: Executive Assistant

Defense Advanced Rsch Proj Agency
ATTN: Dir, Strat Tech Off
ATTN: NMRO
ATTN: Col A. Lowery

Defense Communications Agency
ATTN: Code 510
ATTN: C670

Defense Intelligence Agency
ATTN: DT-1C
ATTN: DI-7D
ATTN: DT-2
ATTN: DB-4C, P. Johnson

Defense Nuclear Agency
ATTN: SPSS
ATTN: SPTD
ATTN: NAFD
ATTN: NATD
ATTN: STNA
ATTN: RAEE
ATTN: NASD
ATTN: STSP
ATTN: STRA
ATTN: NATA
ATTN: RAEV
ATTN: SPAS
ATTN: RAAE
4 cy ATTN: TITL

Defense Technical Info Center
12 cy ATTN: DD

Department of Defense Explo Safety Brd
ATTN: Chairman

Field Command
DNA Det 1
Lawrence Livermore
ATTN: FC-1

Field Command
Defense Nuclear Agency
ATTN: FCTXE
ATTN: FCTT, G. Ganong
ATTN: FCTT, W. Summa
ATTN: FCTX
ATTN: FCTT
ATTN: FCPR
ATTN: FCT

Joint Chiefs of Staff
ATTN: SAGA
ATTN: GD50, J-5 Force Plng & Prog Div
ATTN: GD10, J-5 Nuc & Chem Div

Under Secy of Def for Rsch & Engrg
ATTN: Strat & Space Sys, OS
ATTN: Engrg Tech, J. Persh

DEPARTMENT OF DEFENSE (Continued)

Joint Strat Tgt Planning Staff
ATTN: JPTP
ATTN: JLTW-2
ATTN: JPTM
ATTN: JLA, Threat Applications Div

National Security Agency
ATTN: Director
ATTN: P. Deboy
ATTN: E. Butala

DEPARTMENT OF THE ARMY

Army Logistics Management Ctr
ATTN: Commandant

US Army Electronics R&D Command
ATTN: DELAS-EO, F. Niles
ATTN: DELAS-EO

BMD Advanced Tech Ctr
ATTN: ATC-T
ATTN: ATC-T, M. Capps

BMD Program Office
ATTN: DACS-BMZ
ATTN: Program Manager
ATTN: DACS-BMT

BMD Systems Command
ATTN: BMDSC-HW, R. Dekalb
ATTN: BMDSC-NW
ATTN: BMDSC-HUL, E. Martz
ATTN: BMDATC-R, W. Dickerson
ATTN: BMDSC-H

Chemical Systems Lab
ATTN: J. Andrea

Chief of Engineers
ATTN: DAEN-ZCM
ATTN: DAEN-MPE-T, D. Reynolds
ATTN: DAEN-ZCM, Bernard

Dep Ch of Staff for Ops & Plans
ATTN: DAMO-NCZ

Dep Ch of Staff for Rsch Dev & Acq
ATTN: DAMA-CSS-N, Spt Sys Div, Nuc Tm
ATTN: DAMA-CSM-N

Deputy Ch of Staff for Logistics
ATTN: DALO-ZA

Harry Diamond Labs
ATTN: DELHD-TA-L
ATTN: DELHD-NW-P, J. Gwaltney
ATTN: DELHD-DTSO
ATTN: DELHD-NW-P
ATTN: DELHD-NW-P, F. Balicki

Research & Dev Ctr
ATTN: Commander

US Army Armament Material Readiness Cmd
ATTN: Commander

DEPARTMENT OF THE ARMY (Continued)

DEPARTMENT OF THE NAVY (Continued)

Marine Corps
ATTN: Code POG-31

Naval Civil Engineering Lab
ATTN: Mr. Keenan
ATTN: Naval Construction Bn Ctr
ATTN: Mr. Tancreto

Naval Coastal Systems Lab
ATTN: D. Sheppard
ATTN: Commander

Naval Facilities Engrg Cmd
ATTN: Commander

Naval Material Cmd

DEPARTMENT OF THE AIR FORCE

Aeronautical Systems Division,
ATTN: ASD/ENFTV
ATTN: ASD/ENFTV, D. Ward
ATTN: ASD/ENSG, Capt J. Greneczho

Aerospace Medical Division
ATTN: Commander

Air Force Armament Lab
ATTN: Commander

Air Force Engineering & Svcs Ctr
ATTN: Commander

Air Force Flight Test Ctr
ATTN: Commander

DEPARTMENT OF THE AIR FORCE (Continued)

Ballistic Missile Office
ATTN: ENSN
ATTN: SYDT
ATTN: ENSN, Lt Col Baran
ATTN: Hq Space Div, RST
ATTN: Hq Space Div, RSS
ATTN: ENMR

Deputy Ch of Staff, Rsch, Dev & Acq
ATTN: AFRD

Deputy Chief of Staff
Research, Dev & Acq
ATTN: AFRDQI
ATTN: AFRDS, Space Sys & C3 Dir

Electronic Security Cmd
ATTN: Commander

Electronic Sys Div, OCRS
ATTN: Maj Sugg

Foreign Tech Div
ATTN: Commander
ATTN: PDBG
ATTN: TOPTN
ATTN: TDFBD

Headquarters, US Air Force
ATTN: AFXOOTS

Military Airlift Cmd
A' ': Commander

Rome Air Development Ctr
ATTN: Commander

Space & Missile Test Center
ATTN: Commander

Strat Air Cmd
ATTN: XPFS, Maj Skluzacek
ATTN: XOBM
ATTN: XPQM

OTHER GOVERNMENT AGENCIES (Continued)

US Coast Guard
ATTN: Commandant

DEPARTMENT OF ENERGY CONTRACTORS

University of California
Lawrence Livermore National Lab
ATTN: Director
ATTN: L-262, J. Knox
ATTN: L-8, R. Andrews
ATTN: L-125, J. Keller

Los Alamos National Lab
ATTN: MS 670/T&V
ATTN: J. Hopkins

Oak Ridge National Lab
ATTN: Civ Def Res Proj, Mr Kearny

Sandia National Lab
ATTN: Dept 1100, T. Dowler

DEPARTMENT OF DEFENSE CONTRACTORS

Aerospace Corp
ATTN: R. Crolius

Analytic Services, Inc, ANSER
ATTN: J. Selig

AVCO Systems Div
ATTN: Doc Con

Boeing Aerospace Co
ATTN: M/S 13-13, R. Dyrdahl

Boeing Co
ATTN: M/S 85/20, E. York
ATTN: R. Holmes

California Research & Technology, Inc
ATTN: K. Kreyenhagen

Calspan Corp

DEPARTMENT OF DEFENSE CONTRACTORS (Continued)

Kaman AviDyne
ATTN: N. Hobbs
ATTN: S. Criscione

Kaman Sciences Corp
ATTN: D. Sachs

Kaman Tempo
ATTN: DASIAC
4 cy ATTN: K. Gould

Kaman Tempo
ATTN: G. Perry

Kaman Tempo
ATTN: E. Bryant

Lockheed Missiles & Space Co, Inc
ATTN: F. Borgardt

Lockheed Missiles & Space Co, Inc
ATTN: R. Walz

Lockheed Missiles & Space Co, Inc
ATTN: T. Fortune

Martin Marietta Corp
ATTN: G. Aiello

McDonnell Douglas Corp
ATTN: E. Fitzgerald

National Academy of Sciences
ATTN: National Materials Advisory Brd
ATTN: D. Groves

University of New Mexico
ATTN: G. Lane

Northrop Corp
ATTN: D. Hicks

TRW Electronics & Defense Sector
ATTN: R. Mortensen
ATTN: P. Dai

DEPARTMENT OF DEFENSE CONTRACTORS (Continued)

Pacific-Sierra Research Corp
ATTN: H. Brode, Chairman SAGE

Physics International Co
ATTN: Tech Library

R&D Associates
ATTN: F. Field
ATTN: J. Carpenter
ATTN: P. Haas

S-CUBED
ATTN: R. Duff

Science Applications, Inc
ATTN: J. Manship
ATTN: W. Plows

Science Applications, Inc
ATTN: C. Swain

Science Applications, Inc
ATTN: W. Layson

Southern Research Institute
ATTN: C. Pears

SRI International
ATTN: H. Lindberg
ATTN: A. Burns
ATTN: G. Abrahamson

Teledyne Brown Engineering
ATTN: R. Patrick

Terra Tek, Inc
ATTN: S. Green

TRW Electronics & Defense Sector
ATTN: N. Lipner

Pan Am World Svc, Inc
ATTN: AEDC, Library Doc, TRF

PDA Engineering
ATTN: J. McDonald